CHALMERS
UNIVERSITY OF TECHNOLOGY

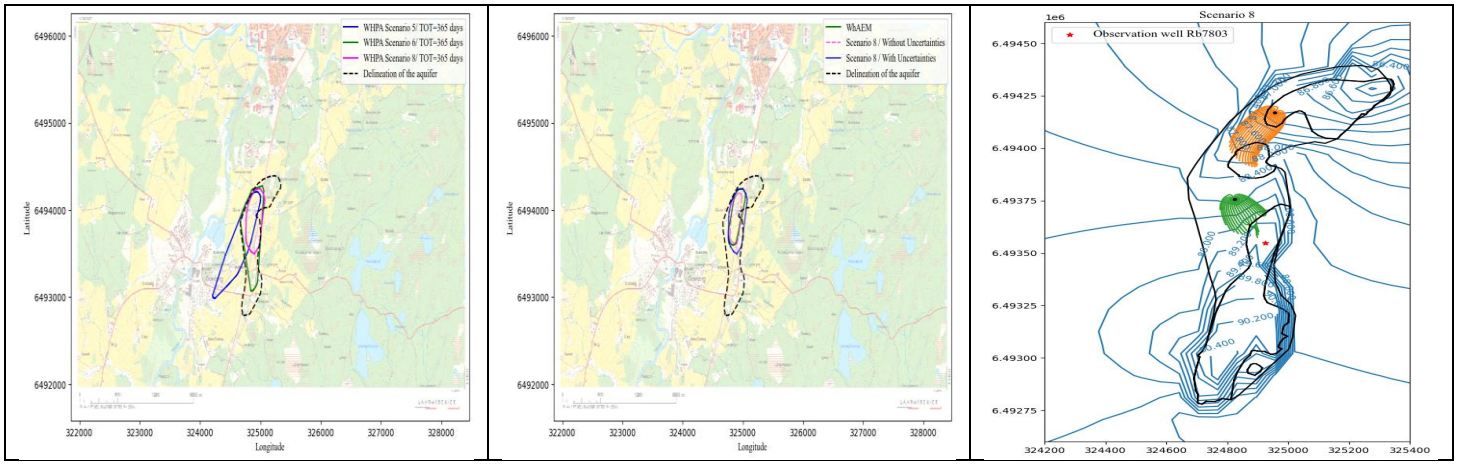

Delineating Drinking Water Protection Areas Using Analytic Element Models (AEMs)

With Focus on Enabling Uncertainty Analysis Using Monte Carlo Simulations

Master's thesis in Infrastructure and Environmental Engineering

MARYAM ZAMZAMI

DEPARTMENT OF ARCHITECTURE AND CIVIL ENGINEERING

CHALMERS UNIVERSITY OF TECHNOLOGY
Gothenburg, Sweden 2023
www.chalmers.se

MASTER'S THESIS ACEX60

Delineating drinking water protection areas with Analytic Element Models (AEMs)

With Focus on Enabling Uncertainty Analysis Using Monte Carlo Simulations

Master's Thesis in Infrastructure and Environmental Engineering

MARYAM ZAMZAMI

CHALMERS
UNIVERSITY OF TECHNOLOGY

Department of Architecture and Civil Engineering
Division of Geology and Geotechnics
Engineering geology
Chalmers University of Technology
Gothenburg, Sweden 2023

Delineating drinking water protection areas with Analytic Element Models (AEMs)
With Focus on Enabling Uncertainty Analysis Using Monte Carlo Simulations

Master's Thesis in Infrastructure and Environmental Engineering
MARYAM ZAMZAMI

Supervisor: Andreas Lindhe, Division of Geology and Geotechnics
Nadine Gärtner, Division of Geology and Geotechnics

Examiner: Lars Rosén, professor in the Division of Geology and Geotechnics

Master's Thesis 2023
Department of Architecture and Civil Engineering
Division of Geology and Geotechnics
Engineering Geology
Chalmers University of Technology
SE-412 96 Gothenburg, Sweden
Telephone: +46 (0)31-772 1000

Cover: Wellhead protection area for the entire aquifer based on the results of TimML and WhAEM.

Printed by Chalmers Reproservice
Gothenburg, Sweden 2023

Delineating drinking water protection areas with Analytic Element Models (AEMs)
With Focus on Enabling Uncertainty Analysis Using Monte Carlo Simulations

MARYAM ZAMZAMI
Department of Architecture and Civil Engineering
Chalmers University of Technology

Abstract

The delineation of a wellhead protection area (WHPA) is a crucial task aimed at safeguarding underground water resources. There are various methods available to achieve this, ranging from simple approaches like fixed radius estimation with inherent limitations to more sophisticated numerical models, which are considered the most detailed and reliable but time-consuming and data-intensive option. An analytical element model (AEM) provides a middle ground between these two extremes, offering users the flexibility to implement different boundary scenarios without being constrained by grid limitations. Moreover, AEM can perform better in cases where data is scarce. However, it is important to recognize that the output of groundwater modeling can never be claimed to fully reflect reality due to inherent uncertainties. These uncertainties arise from various sources, including conceptual understanding, model simplifications, and lack of data. To address these uncertainties, TimML, a multi-layer, analytic element model, is employed and further enhanced to enable Monte Carlo Simulations (MCS). To evaluate the effectiveness of the approach, a case study was selected in which eight different scenarios were considered and caclualtions performed using MCS to consider uncertainties. The calculated ranges of protection zones from these scenarios are illustrated for the study area and benchmarked against the outcomes of the wellhead analytical element model (WhAEM), an existing software for delineation of WHPAs tht does not enable MCS. The results from the TimML model illustrates the added value of considering parameter ucnertainties and how it affects the WHPA. Furthermore, the comparison reveals that the largest differences are between the different scenarios rather than the two applied models. This emphasizes the significant role of uncertainties arising from different assumptions in the case study, highlighting that stochastic modeling alone is not sufficient to capture all relevant uncertainties.

Keywords: groundwater modeling, analytic element model, uncertainties, water protection, Monte Carlo analysis, stochastic modeling

Acknowledgments

This thesis was conducted at Chalmers University of Technology in the autumn of 2022 and spring 2023. I am grateful to my supervisors, Andreas Lindhe and Nadine Gärtner, for introducing me to this fascinating research topic and for providing valuable guidance throughout the process. The thesis has provided me with valuable insights into the diverse range of uncertainties and challenges involved in groundwater modeling. I would like to express my sincere appreciation to Lars Rosén, my examiner, and Erik Toller, Ph.D. at Uppsala University, for their dedicated efforts and time invested in this thesis, as well as for generously sharing their expertise and knowledge. I am also grateful to Lars-Ove Lång at SGU, and Tony Grantz along with all the other employees at Västvatten, for their assistance and provision of necessary materials. Lastly, I extend my heartfelt gratitude to my family for their unwavering support throughout my Master's journey. Their encouragement and belief in me have been invaluable.

Maryam Zamzami
Gothenburg, Sweden, July 2023

Table of Contents

List of Figures

List of Tables

1

Introduction

This chapter includes a general introduction to the topic of this study. The background and motivation for carrying out the study are presented, as well as the aim of the project and the outline of the thesis.

1.1 Background

Access to safe and clean drinking water is considered one of the fundamental necessities for human life. Due to demographic and environmental transformations such as population growth, urbanization, and desertification, along with an increase in consumption driven by economic expansion, the availability of the world's water resources is limited and facing growing strain. The intensification of this scarcity in the future is inevitable. Moreover, the challenges are further complicated by the impacts of climate change, which is already causing an unprecedented rate of change in the global water cycle. This is evident through the altered timing, intensity, and unpredictability of rainfall, droughts, and flooding events. Therefore, sustainable protection and management of water resources have emerged as a top concern for the future (The Swedish Research Council Formas, 2009).

Freshwater only constitutes 3% of the total water existing on the earth. This is including glaciers, atmospheric water, groundwater, and surface water. Among the named resources, surface, and groundwater are the primary sources of drinking water for society due to ease of access (Bureau of Reclamation California-Great Basin, 2020). Similar to surface water, the recharge of groundwater is primarily dependent on precipitation and runoff events, although its dynamics make it resilient to droughts and other hydrologic events. This characteristic makes groundwater a crucial water source for securing access to water. Furthermore, given that the water supply in many areas heavily relies on surface water, scarcity not only necessitates securing the water supply but also elevates the value of groundwater. To harness the value of groundwater, it is imperative to implement effective management practices that ensure its sustainable use. When managed appropriately, groundwater resources can serve as renewable sources, offering long-term viability and reliability (Kraemer et al., 2000; Vaux, 2011).

Globally, there has been a notable rise in the reliance on groundwater sources because of the rapid decline in the quality of surface water brought on by population growth. Both rural regions and fast-growing urban areas may attest to this (The Swedish Research Council Formas, 2009). Since groundwater is generally free from infectious microbes – aquifer media and soil cover with biological activity are natural barriers to microbial contaminants (Kraemer et al., 2000)– utilizing it as a freshwater resource has several benefits over surface water. Nevertheless, the quality of groundwater intended for human consumption may differ based on its origin and often requires vigilant monitoring. Furthermore, remediation of groundwater resources when contamination is detected poses difficult hurdles (The Swedish Research Council Formas, 2009).

An effective and economic way to protect groundwater resources from potential hazardous events is the prevention of pollution penetration into the aquifer rather than subsequent remediation (Vaux, 2011). Often, pump and treat technologies are the only options when it comes to groundwater clean-up. While utilizing a preventive and risk-based strategy is

advocated within the water industry (WHO, 2017) and the overwhelming body of data supports the necessity for groundwater protection schemes (Kraemer et al., 2000), there has been no assurance that such plans will be successful. Nevertheless, the management of groundwater resources responsibly and efficiently is imperative during a time of increasing scarcity (Vaux, 2011).

To protect groundwater sources, designated zones known as Wellhead Protection Areas (WHPAs) are established. These zones are defined as "the surface and subsurface area surrounding a water well or wellfield that supplies a public water system and through which contaminants are reasonably likely to move toward and reach such a water well or wellfield" (U.S. EPA, 1987). WHPA delineation can be achieved using different methods, but uncertainties arising from input parameters, boundary conditions, and model structure must be addressed (Højberg & Refsgaard, 2005). The lack of data exacerbates these uncertainties, making it necessary to explore new approaches that can provide decision support for accurate WHPA delineation.

1.2 Motivation

Groundwater modeling is crucial for managing and assessing drinking water resources. However, the lack of data introduces uncertainties in the model, undermining the accuracy of the results. To enhance the reliability of groundwater models used in WHPA delineation, it is essential to develop methods that address these uncertainties. By identifying and mitigating sources of uncertainty, we can improve the accuracy of WHPA delineation and provide reliable decision support for groundwater management.

1.3 Aim and Objectives

The aim of this study is to develop an integrated model for the delineation of WHPAs by implementing Monte Carlo simulations (MCS) in TimML, a multi-layer analytic element model (AEM) Python-based code. This model addresses parameter uncertainties and incorporates multiple conceptual models to account for uncertainties in hydrogeological interpretations. The developed code enables the delineation of WHPAs considering uncertainties in a structured manner without the need for numerical modeling. The study further aims to perform a comprehensive case study to evaluate the practical application of the developed model and assess its effectiveness in enhancing the safeguarding of groundwater catchment areas. The specific objectives of the study are as follows:

1) Implementing MCS in TimML to address uncertainties and enhance the reliability of the WHPA delineation model
2) Conduct a case study to assess the practical utility of the developed model in a real-world scenario
3) Compare the results obtained from the developed model with those derived from an established model to evaluate the suitability and robustness of the framework

1.4 General limitation

As with any study, certain limitations should be acknowledged. In this case, it is important to note that the study is based on a single case study area, which may limit the generalizability of the findings.

1.5 Thesis outline

This thesis is divided into 8 chapters to give a clear understanding of the topic to the reader. Chapter 1 is a brief introduction to the WHPA concept, the method used to carry out the project as well as the aim and the idea behind the thesis. In Chapter 2, a more detailed and technical background regarding WPA, AEM, and Monte Carlo is provided. Furthermore, a literature review to find the suitable method and the related work done in this domain is presented. Chapter 3 is dedicated to a brief description of the case study and its characteristics. Chapter 4 includes the utilized methodology for the study followed by the results and discussion, in Chapters 5 and 6, respectively. The conclusion of the carried-out study is presented in Chapter 7.

2

Theoretical Background

This chapter provides the theoretical underpinnings for some of the main concepts that are used in this study namely, groundwater principles, water protection areas (WPAs), modeling, numerical models, analytic element models (AEMs), uncertainty, and Monte Carlo Simulation (MCS).

2.1 Water Protection Areas (WPAs)

To safeguard the water resources from potential contamination and provide high-quality potable water, the concept of water protection areas (WPAs) that encompasses all types of water sources, was introduced (SwAM, 2021). In the case of public drinking water wells the term wellhead protection areas (WHPAs), which aim to protect groundwater resources from potentially polluting activities to reach the pumping well by imposing restrictions, is used internationally (U.S. EPA, 1987). WHPA consists of zones where regulation of activities, especially human activities, such as the usage of pesticides and fertilizers, which can degrade the quality of water, is necessary to avoid unacceptable risks to the water source (U.S. EPA, 1987).

Based on the Great Britain Environmental Agency report (Carey et al., 2009) and Sweden's previous handbook for water protection areas (SEPA, 2011), WHPA can be classified into three main source protection zones (SPZs) with different times of travel (TOT). The primary or inner protection zone is the most sensitive area which is located adjacent to the well where an ample amount of time for the decay of biodegradable substances and water-borne disease is considered. By providing a minimum TOT for slow-decaying pollutants, the outer tier known as the secondary protection zone, allows the attenuation of these contaminants to reach a permissible concentration. The tertiary protection zone, referred to as the source catchment protection area, guarantees the long-term sustainability of the water wells as in this region it is assumed that all groundwater recharge is discharged at the source (see Figure 2-1).

Although using TOT for the WHPA delineation is the most common criterium all around the world, the U.S. EPA (U.S. EPA, 1987 & 1994) considers 5 criteria that can be applied either as a single or in combination. In Table 2-1, these criteria and the WHPA methods that utilize them are represented. It should be noted that SEPA (SEPA, 2011) also highlights the significance of employing a risk-based approach while emphasizing the continued relevance of TOT as a fundamental criterion for defining appropriate zones. The TOT method is justified as protecting groundwater resources because: 1) the given mean time gives the non-conservative pollutants the chance to be assimilated, or 2) the responsible community has enough time to develop a response plan in the case of spotting any conservative contaminations in the protection zone. Particles that are susceptible to sorption or transformation processes are referred to as conservative contaminants (Kraemer et al., 2000).

Various methods have been introduced for the delineation of the WHPAs some of which can be seen in Table 2-1; however, they can be classified into three major categories (Staboultzidis et al., 2017):

A) an arbitrary or calculated fixed radius (by assuming a 1D equation) around the well, a method that may overestimate or underestimate the protection areas considerably.

B) analytic element methods (AEMs), and

C) numerical methods.

Approaches B and C are further elaborated in this report.

Based on the conclusion reached by Liu et al. (2019), it is advised that WHPA delineation should be based on reducing the complexity of groundwater flow systems as much as possible so that nationwide program implementation is simplified, while still preserving the crucial geological and hydrological characteristics that ensure effective groundwater protection.

Table 2-1. WHPA delineation criteria and methods (Kraemer et al., 2000)

Criteria \ Methods	Arbitrary fixed radius	Calculated fixed radius	Well in a uniform flow field	Hydrogeologic mapping	Hydrogeologic modeling	Transport/transformation modeling
Distance	X	X				
Drawdown		X	X		X	X
Time of travel		X	X		X	X
Flow boundaries				X	X	X
Assimilative capability						X

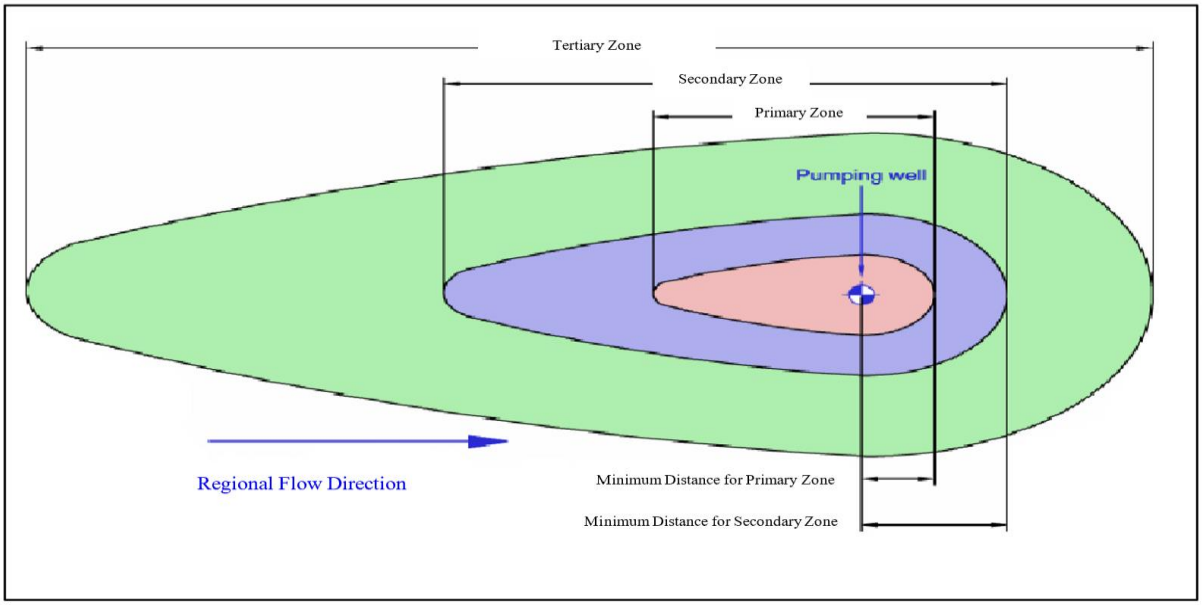

Figure 2-1. Schematic representation of primary, secondary, and tertiary catchment protection zones (Carey et al., 2009)

2.2 Basic principles of groundwater flow

2.2.1 Hydraulic gradient (i)

The non-stationary characteristic of the groundwater is not only a response to the force of gravity on a slope but also due to the difference of hydrostatic and lithostatic pressures at the recharge and discharge zone. The groundwater gradient refers to the incline of the water table, which dictates the average velocity of the flow and its direction. Essentially, the steeper the gradient, the faster the groundwater will move, and it generally flows in the direction of the steepest gradient. Mathematically, i is defined as the changes in total head per unit distance (Cromer, 2013).

$$i = \frac{\Delta h}{\Delta l} \qquad \text{Equation 2.1}$$

2.2.2 Effective Porosity (n_e)

Effective porosity is defined as the percentage of the volume of interconnected pore spaces (V_I) – which form the groundwater flow path – to the total volume (V) as defined in Equation 2.2. The reason why porosity is highly important in hydrogeology is that the value of the porosity can give an insight into the soil's permeability and its capacity to store water (Fetter, 2014). Moreover, information about the soil's particle size and texture in the absence of consolidation can be obtained (Larum, 2021; Woessner & Poeter, 2020).

$$n_e = \frac{100\ V_I}{V} \qquad \text{Equation 2.2}$$

2.2.3 Groundwater discharge

Water flow in a soil profile obeys Darcy's law Equation 2.3 based on which groundwater discharge (Q) is proportional to the hydraulic gradient (i), cross-section (A) of the profile, and a constant parameter known as hydraulic conductivity (K), which indicates how easily water transmits through the aquifer media (Cromer, 2013) and is dependent on both the fluid (in this case water) and soil material characteristics. The validity of Darcy's law is determined by laminar flow (when the velocity of the flow is small) which is true in natural groundwater (Fetter, 2014).

$$Q = -\mathrm{KA}\ \frac{\Delta h}{\Delta l} \qquad \text{Equation 2.3}$$

2.3 Modeling

To anticipate the behavior of a physical system over a period, a model can be used. Practical modeling embraces a step-by-step manner of solving a problem. Models can be classified as conceptual, physical, or mathematical (Kraemer et al., 2000; Sikdar, 2019). General principles, which are formed from groundwater flow processes and boundary conditions, are used to represent a system in a conceptual model. A physical model is a scaled-down replica of a real system. An illustration of a system using mathematical concepts and terminology is called a mathematical model (Kraemer et al., 2000; Sikdar, 2019). Therefore, a model is only a simplification of the reality which is designed to represent a problem following the aims and objectives of the specific task or analysis being performed (Kraemer et al., 2000).

Mathematical models include analytical and numerical models. Analytical models have a closed-form solution that can be stated as a mathematical analytic function, whereas numerical models use a numerical time-stepping procedure to analyze the behavior of the model over time. Hydrogeologists and civil engineers employ the concept of groundwater modeling to simulate the behavior of an aquifer system by describing its fundamental characteristics in a carefully regulated physical or mathematical manner. Groundwater models have shown to be effective tools for addressing many groundwater issues, even though they are not ideal and merely reflect a simplified form of a complex aquifer system. They offer insight into the behavior of a groundwater system (GS) with an acceptable degree of confidence (Sikdar, 2019).

The effective management of groundwater resources necessitates the inclusion of groundwater modeling in the decision-making process for groundwater development projects, as it plays a pivotal role in ensuring the sustainable utilization of these valuable resources. Groundwater models can be used to interpret groundwater flow patterns and pollutant transport, forecast changes in head or pollutant concentration in response to future stress, examine groundwater recharge, discharge, and storage, and visually communicate important messages to the public and decision-makers (Sikdar, 2019).

2.4 Numerical Models

As mentioned earlier, a mathematical model can be solved using either a numerical or analytical approach. Although the focus of this report is on analytical models, a brief description of numerical models is presented in this section. For additional information on this method, the reader is referred to Sikdar (2019) and Anderson et al. (2015).

The partial differential equation that describes groundwater flow in porous media can be solved effectively by numerical modeling. In this model, the mentioned equation which is derived from Darcy's law and addresses the conservation of mass principle Equation 2.4) is mostly solved for the head. Numerical models can solve the complete transient, 3D, heterogeneous, and anisotropic equations under complicated boundary and initial conditions, even though they only use approximation representations of the governing equation. The answers offered by numerical models are computed at discrete locations or nodes rather than being continuous in space or time. The finite-difference (FD) approach and the finite-element (FE) method are the two numerical techniques that are most frequently employed in groundwater modeling. Both approaches strive to produce a reasonably close approximation of the solutions rather than exact solutions, although they are both frequently used and are efficient in generating accurate results (Anderson et al., 2015; Sikdar, 2019).

$$\frac{\partial}{\partial x}\left(K_x \frac{\partial h}{\partial x}\right) + \frac{\partial}{\partial y}\left(K_y \frac{\partial h}{\partial y}\right) + \frac{\partial}{\partial z}\left(K_z \frac{\partial h}{\partial z}\right) + W = S_s \frac{\partial h}{\partial t} \qquad \text{Equation 2.4}$$

Where:

K_x, K_y, *and* K_z are hydraulic conductivities in the *x*, *y*, and *z* directions, respectively
h is hydraulic head
W is volumetric flux per unit volume
S_s represents specific storage
t is time

In case of a steady state condition the last term ($S_s \frac{\partial h}{\partial t}$) will be zero.

The existing numerical methods such as FD and FE solutions have restrictions in terms of their applicability in large areas and the reason behind this limitation is that:

1) the continuity of flow is not guaranteed and must be checked each time,

2) the definition of the groundwater flow is in terms of head and therefore restricted to the grids and nodes, in other words, to find the head in locations where there are no grids, interpolation is needed.

These inaccuracies may lead to numerical dispersion which only can be minimized by refining the grids or element network (H.M. Haitjema, 1995).

2.5 Analytic Element Model (AEM)

The analytic element model (AEM) is a mathematical approach for modeling the flow of groundwater under hydrological conditions (Kraemer et al., 2000), in which a solution is achieved through the combination of several hundred elementary analytic solutions (Badv & Deriszadeh, 2005). To accurately depict each hydrologic feature, for instance, a river, an analytical element is employed, which is associated with mathematical functions (Badv & Deriszadeh, 2005; Kraemer et al., 2000). This indicates that each element corresponds to a hydrogeologic feature. For example, the geometry of a meandering stream can be approximated by a string of straight-line elements. At the background of each of these elements, a function can be found that determines the movement of the groundwater into or out of that specific stream. This function which is called a “line-sink function” can be visualized as a finite line formed by combining an infinite number of point sinks (Kraemer et al., 2000). A sink refers to a location where fluid is unceasingly and uniformly drawn off (Zhivov et al., 2020).

AEM was first developed to solve regional flow problems and unlike numerical modeling, it provides an approximate numerical solution that isn't limited to the grids of the studied area (see Figure 2-2), which means the avoidance of discretization of the groundwater flow. Thus, the method allows the user direct entry of hydrogeological and geological inputs. The absence of grids or element networks makes this model flexible enough for the seamless integration of various boundary conditions within a single model. For instance, the use of line-sink to create river and lake boundaries, areal sinks to model recharge areas, and line sink with a bottom resistance to represent streams and lakes that are partially connected to the aquifer (Badv & Deriszadeh, 2005). Furthermore, inhomogeneity can be addressed through the application of line doublets or double layers (H.M. Haitjema, 1995). Moreover, the characteristic of being grid-independent removes the need for agreement between model resolution and the area size. The scale-insensitivity of AEM can be attributed to this reason. Therefore, the spatial scope of AEM is not a constraint, but rather the amount of detail represented (Badv & Deriszadeh, 2005; H.M. Haitjema, 1995).

The AEM can be applied to multi-aquifer systems that have a steady flow, piecewise constant system parameters, and leaky layer characteristics. This approach is based on the superposition of a partial differential equation (PDE), which defines the unknown function based on multi-independent variables and its partial derivative relative to those variables. Therefore, AEM gives an exact solution to governing PDE. Inaccurate groundwater flow velocities will not

cause numerical dispersion since heads and groundwater flow velocities can be determined at any place within the flow domain (Badv & Deriszadeh, 2005; H.M. Haitjema, 1995).

In addition to solving internal boundary issues in both finite and infinite domains, the AEM can also replicate flow at both local and regional levels, as demonstrated by its use in modeling the impact of the Tennessee-Tombigbee Waterway on adjacent aquifers (Strack, 2003). In AEM, the groundwater time-of-travel (TOT) is calculated and used as the delineation criterion.

On the other hand, some drawbacks make this method unpopular worldwide. Firstly, as the linearity of a problem allows the use of superposition, which is the basis of the AEM, the method is not applicable in case of any heterogeneity or anisotropy (H.M. Haitjema, 1995). Although this problem has been addressed in newly available codes (Bakker, 2006), compared to FD or FE method which can easily accommodate these characteristics, AEM requires proficiency in handling sophisticated mathematical equations, demanding advanced skills in mathematics for their successful implementation (H.M. Haitjema, 1995). Secondly, because AEM is typically based on complex equations, it necessitates further simplifications of the flow system, and therefore more assumptions. A few examples include disregarding vertical flow and treating the aquifer as a horizontal system or applying uniform conductivity to the entire system. Therefore, addressing transient flow, 3D unconfined aquifer, and 3D multilayer is computationally expensive and limited in this model.

However, it should be noted that collecting data is time-consuming and expensive, and there is there will always be uncertainties related to parameters such as recharge rates and spatial distribution of conductivity. As a result, hydrogeologists find the AME model appealing because it requires relatively fewer input data than the numerical model (H.M. Haitjema, 1995).

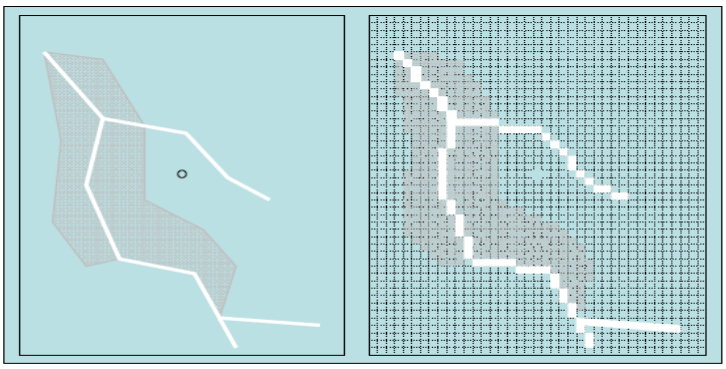

Figure 2-2. Analytic element model vs finite-difference (Craig, n.d.)

2.5.1 Mathematical background

In this section, which is mainly based on Bakker & Kelson (2009), Craig, H.M. Haitjema, (1995), and Strack (1989), the mathematical equations and principles that are common in defining the single confined aquifer in the AEM are presented as an illustrative example to demonstrate the functionality of an AEM model. For the detailed description and formulation, readers are encouraged to look at the mentioned references.

Reaching an equation for solving the current groundwater problem is possible through the superimposition of numerous individual solutions for each linear partial differential equation

(PDE), such as the Laplace equation ($\nabla^2\Phi = 0$), Poisson equation ($\nabla^2\Phi = -N$), Helmholtz equation ($\nabla^2\Phi = {\Phi}/{\lambda^2}$), etc. (Craig, n.d.). As the horizontal direction of the flow is dominant in groundwater movement, Equation 2.4 can be written as a 2D equation as follow (Craig, n.d.):

$$\frac{\partial}{\partial x}\left(K_x H \frac{\partial h}{\partial x}\right) + \frac{\partial}{\partial y}\left(K_y H \frac{\partial h}{\partial y}\right) = -N + S\frac{\partial h}{\partial t} \qquad \text{Equation 2.5}$$

Where:

H is the aquifer saturated thickness,
N represents the vertical influx such as recharge or leakage, and
S is the storage coefficient

The integrated discharge in the *x* and *y* directions can be defined as (Craig, n.d.):

$$Q_x = K_x b\frac{\partial h}{\partial x} \quad \& \quad Q_y = K_y b\frac{\partial h}{\partial y} \qquad \text{Equation 2.6}$$

Equation 2.5 is known as the Dupuit-Forchheimer approximation which is based on the following assumptions (H.M. Haitjema, 1995):

1. Regional flowlines are primarily horizontal, and velocities are constant throughout the depth of the aquifer (converting 3D to a 2D model)
2. The negligibility of vertical gradients in the head ($dh/dx \approx 0$) suggests that the average value of the head serves as a suitable representation of it
3. In the vertical direction, flow resistance is insignificant ($K_z \approx 0$)
4. The vertical specific discharge (q_z) can be calculated by applying mass balance rather than Darcy's law
5. Suitable for situations where the flowline length is greater than the aquifer thickness (also known as shallow aquifers), as is the case with most of the groundwater flow concerns related to water resources problems.

It should be mentioned that in the Dupuit-Forchheimer equation, the water balance is not changing (see Figure 2-3), while the head distribution in the vertical direction is neglected. Analytical element formulations are frequently expressed in terms of a discharge potential (Φ). Therefore, to solve Equation 2.5 by assuming an isotropic and homogeneous aquifer, Φ can be defined as (Craig, n.d.):

$$\begin{gathered}\text{Confined aquifer: } \Phi = KHh - \tfrac{1}{2}KH^2 \text{ (b} \geq \text{H)} \\ \text{Unconfined aquifer: } \Phi = \tfrac{1}{2}KH^2 \text{ (b} < \text{H)}\end{gathered} \qquad \text{Equation 2.7}$$

The relation between integrated discharge and discharge potential is (see Figure 2-3):

$$Q_x = -\frac{\partial \Phi}{\partial x} \quad \& \quad Q_y = -\frac{\partial \Phi}{\partial y} \qquad \text{Equation 2.8}$$

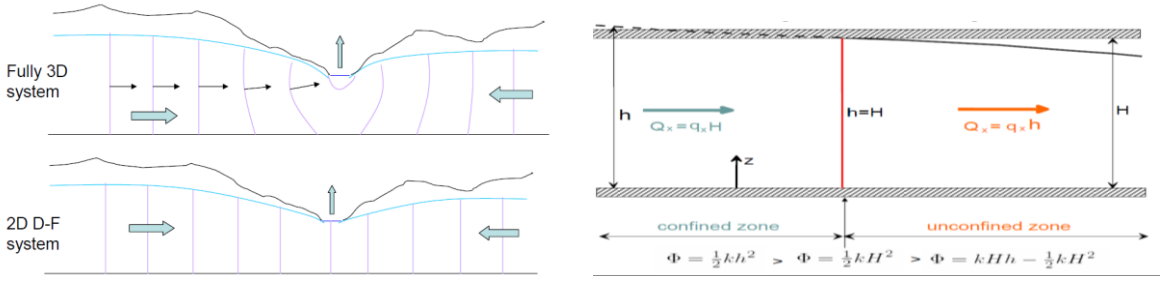

(a) (b)

Figure 2-3. a) Converting a 3D system to a 2D system, and b) integrated discharge (Craig, n.d.)

By assuming a steady flow and combining Equation 2.6 and Equation 2.8, the governing equation can be rewritten as follows (Craig, n.d.):

$$\frac{\partial^2 \Phi}{\partial x^2} + \frac{\partial^2 \Phi}{\partial y^2} = \nabla^2 \Phi = -N \qquad \text{Equation 2.9}$$

For steady confined Dupuit-Forchheimer flow in a homogeneous aquifer Φ is equal to the head (h) times the transmissivity (T):

$$\Phi = Th \qquad \text{Equation 2.10}$$

The Potential Φ satisfies Laplace's differential equation when there is no local recharge. As it was mentioned previously, AEM is a composite of analytic functions that are also referred to as elements with at least one degree of freedom. Assuming only one free parameter for every element and a cartesian (x, y) coordinate system to make the calculations simpler, the potential can be defined as follow (Bakker & Kelson, 2009):

$$\Phi(x,y) = \sum_{i=1}^{N} p_i \Phi_i(x,y) \qquad \text{Equation 2.11}$$

In Equation 2.11, N is the total number of analytical elements, p_i stands for the i^{th} element's free parameter, and Φ_i is the i^{th} element's unit-influence function. Superposition of elements can also be applied in the presence of areal recharge. The potential can be written as Equation 2.12 by consideration of N_w wells with the uniform flow and p_0 as an additive constant (Bakker & Kelson, 2009):

$$\Phi(x,y) = \sum_{i=1}^{N_w} p_{w,i} \Phi_{w,i}(x,y) + p_u \Phi_u(x,y) + p_0 \Phi_0 \qquad \text{Equation 2.12}$$

The Thiem solution for a unit discharge, where $p_{w,i}$ is the i^{th} well discharge and $\Phi_{w,i}$ is the i^{th} well potential influence, is represented by this equation. As each well has a specific location, the $\Phi_{w,i}$ can be defined as (Bakker & Kelson, 2009):

$$\Phi_{w,i} = \frac{1}{4\pi} \ln\left[(x - x_i)^2 + (y - y_i)^2\right] \qquad \text{Equation 2.13}$$

In this equation, (x_i, y_i) represents the location of the i^{th} well. Also, the term $p_u\Phi_u$ in Equation 2.12 is a uniform flow in which the potential influence and the multiplication of regional hydraulic gradient and transmissivity are represented by Φ_u and p_u respectively. In cases where potential influence makes an angle (α) with the positive x direction, it can be defined as follow (Bakker & Kelson, 2009):

$$\Phi_u = -x\cos(\alpha) - y\sin(\alpha) \qquad \text{Equation 2.14}$$

Finally, in the constant term $p_0\Phi_0$ of Equation 2.12, Φ_0 is equal to unity and p_0 can be calculated by choosing calibration targets, for example, head or flux.

2.5.2 Types of elements

The behavior of the groundwater flow regime can be altered due to interaction with surface water, changes in the aquifer's properties, and infiltration of precipitation. In AEM each of these hydrogeological features can be modeled (see Figure 2-4) using a specific element, in this case, line sinks, line doublets, and areal sinks, respectively (H.M. Haitjema, 1995). These elements are briefly presented in the following sections.

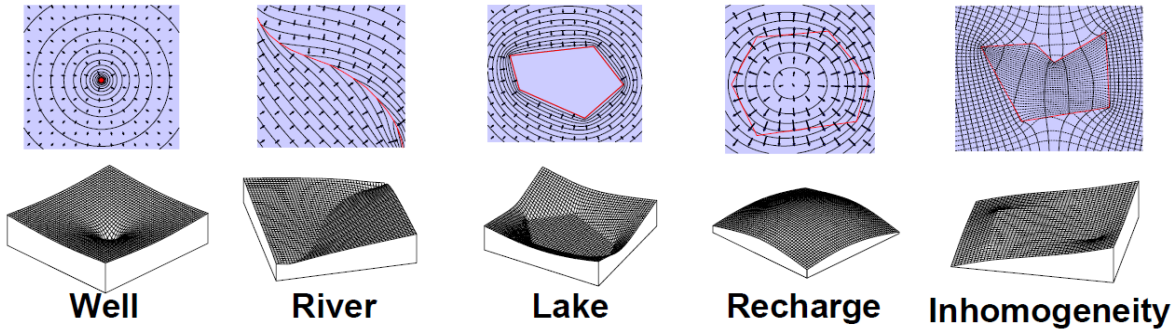

Figure 2-4. Analytic elements (Craig, n.d.)

2.5.2.1 Line sinks

As it was mentioned previously, to model a surface water feature such as a stream or boundary of a wetland- e.g., a lake- that feature will be split into numerous segments, each called a line sink (see Figure 2-5). The sink density of the line-sink corresponds to the amount of groundwater that enters or exists in that segment of the stream. Therefore, the differentiation in sink densities is due to the distinct groundwater infiltration rate in each segment. Positive and negative sink densities can be applied to gaining and losing stream segments, respectively. The term gaining streams is used when the stream is recharged by the groundwater (H.M. Haitjema, 1995; Kraemer et al., 2000). Sink densities are not predetermined but can be calculated by solving a set of linear equations which are based on known head beneath the surface water feature section (Kraemer et al., 2000), since based on the Dupuit-Forchheimer assumption, mentioned previously, the water level in the modeled feature is the same as the hydraulic head in the aquifer located beneath it (H.M. Haitjema, 1995).

Line-sinks along lake boundaries imply groundwater interaction only occurs at the lake edges, which conveys an appropriate approximation of reality regarding the exchange when the surface water feature is large compared to aquifer saturated thickness. For wide rivers and

streams, adding line-sinks on both sides can make the model more realistic (Kraemer et al., 2000). The number of modeled line sinks depends on two factors: the requirement for (1) detailed geometry and (2) variations in groundwater discharge or recharge. More line-sinks are necessary for accurate representation in the immediate area of interest, known as the near field, particularly in proximity to high-capacity wells (Kraemer et al., 2000).

2.5.2.2 Line doublets

On a regional scale, aquifer properties vary across different areas, which is primarily due to alterations in geology. For instance, variation in the grain size distribution can result in inhomogeneous porosity and hydraulic conductivity. A closed form of line doublets can be applied to consider these inhomogeneities. Commonly referred to as a double layer, a line doublet consists of two layers of singularities. This element can be visualized as a close alignment of a line sink and a line source (see Figure 2-5), where their discharge and recharge rates are simultaneously increased to an infinitely large value while maintaining equality. Consequently, while maintaining flow continuity, a polygon line doublet can produce a jump in discharge potential (H.M. Haitjema, 1995).

Furthermore, it should be mentioned that as it is difficult to gather information on aquifer thicknesses and hydraulic conductivities, surface geology maps and well logs can be utilized to detect aquifer inhomogeneities. To obtain a more accurate prediction of regional groundwater flow, it is important to model inhomogeneities in the near field with more specific details (H.M. Haitjema, 1995).

2.5.2.3 Areal sinks

A source disk with a circular shape can be used to represent an irrigation area or a pond. Using this feature to model the areal recharge caused by precipitation requires changes as the geology of the area can affect the recharge rate. For instance, in a case of a sandy aquifer constrained by clay material, sand facilitates a greater rate of precipitation in comparison to clay. The mentioned alteration can be satisfied by the introduction of an areal sink element to the model. An areal sink which can either be a polygon or a circular shape, fulfills the Laplace equation and Poisson equation outside and within its boundary, respectively (see Figure 2-5).

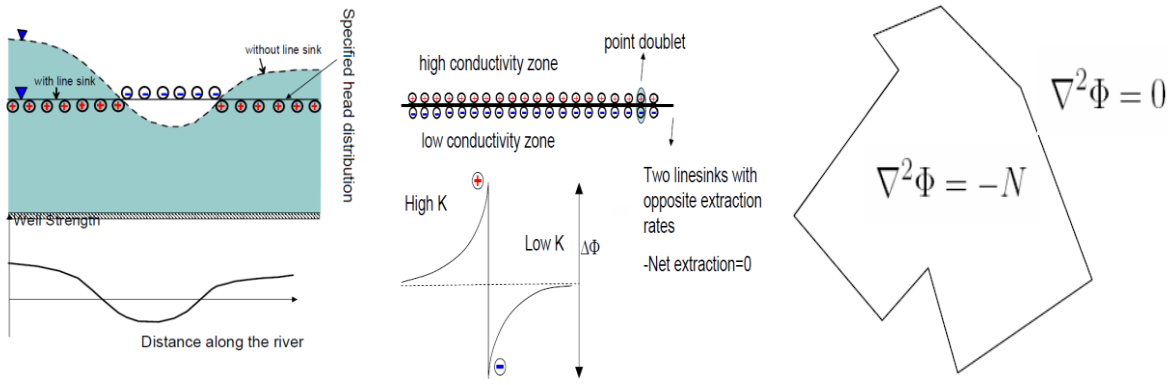

(a) (b) (c)

Figure 2-5. Analytic elements a) line sink, b) line doublet, and c) areal sink (Craig, n.d.)

2.5.3 Applications of AEM

In the article" Using Analytic Element Models to Delineate Drinking Water Source Protection Areas" by Raymond et al. (2006), the authors describe that the AEM can fill the gap between the simple methods and more sophisticated numerical methods for the delineation of WHPAs. By testing AEM on more than 535 public water systems, the Ohio EPA hydrogeology department has introduced AEM as a relatively easy developing method. Furthermore, through a comparison of the results with numerical methods, it has been confirmed that AEM is capable of producing satisfactory delineations of protection zones, while both the size and the shape of WHPA are significantly different in a simpler method like fixed reduce strategy.

Numerous studies have demonstrated that the results of an AEM for the delineation of WHPAs are comparable to those of more sophisticated techniques like the FD model (Liu et al., 2019; Nikiel & Zdechlik, 2022; Raymond et al., 2006). Also, the acceptable complication and time to obtain the results have made the AEM a powerful alternative to complex numerical models (Hunt, 2006; Nikiel & Zdechlik, 2022). Numerous published articles introduced AEM as the semi-analytical method which is different from the analytical method. Following, some works that have been done in this scope are presented in ascending yearly order.

In CSOMA (2001), cases, where AEM can preferably be used, were presented. One of these cases is when there is uncertainty in the boundary condition due to limited data and accuracy in local and regional modeling, especially when groundwater levels fluctuate. Unlike the FD method, which requires clearly defined boundary conditions around the study area, AEM only needs the outer boundaries.

In another study published by Staboultzidis et al. (2017), an analytical element method was used for the delineation of WHPA in the Agia aquifer, Greece. By implementing three different scenarios (wet, dry, and annual averaged), it was concluded that the aquifer current protection zone, which is based on a fixed radius method, does not necessarily prove the needed protection for the studied groundwater resource. Furthermore, it was mentioned that the lack of data, time constraints, and the size of the catchment were the reasons behind the choice of AEM.

In their study of an unconfined aquifer in Israel, Liu et al. (2019) compared various WHPA delineation techniques to the numerical model, which was used as the reference. It was determined that the semi-analytical approach WhAEM, which is based on the AEM concept, is the only one that can produce findings that are acceptable and consistent with the numerical model. Further exploration was conducted on the implementation of stochastic modeling to account for the uncertainties in the numerical model. This approach aimed to generate a probabilistic distribution of WHPAs, considering uncertain input hydrogeological parameters, instead of relying solely on a deterministic protection zone.

2.5.4 AEM software

In this section, two software options for modeling AEM are described:

2.5.4.1 TimML

To implement AEM in a programming language environment, an object-oriented and flexible computer program known as TimML 6.0 can be employed. The older versions of this program used to be a combination of Python and FORTRAN scripts, while the current version is only coded in Python and uses "numba", a compiler that accelerates the performance of the code.

This program is used for modeling steady-state multi-layer flow and there is no limitation on the number of leaky layers or aquifers to which TimML can be applied. The model can calculate head, flow, and leakage among different layers of the aquifer at any point. However, it is important to note that the current code does not incorporate stochastic modeling, and therefore, there is a need for further development of the code to enable the implementation of uncertainty and sensitivity analysis.

TimML is a beneficial choice for modeling since it is based on Python, an open-source package. This open-source nature allows for further development and customization based on users' needs, making TimML a versatile tool for various modeling scenarios.

2.5.4.2 WhAEM

The application of the U.S. EPA's groundwater hydrogeology computer program wellhead analytic element model (WhAEM) software allows the facilitation of the delineation of WHPAs. With the use of various techniques including, radius approaches, well-in-uniform flow solutions, and geohydrologic modeling techniques (steady state flow), WhAEM2000 offers an interactive user interface for designing groundwater protection areas (Badv & Deriszadeh, 2005).

2.6 Uncertainties

A groundwater system (GS) and its characterization will always be incomplete as most of the subsurface is unseen. An approach to have a better understanding of GS is the creation of links among the pointwise data while securing their temporal and spatial continuity by the application of the models (Ramgraber & Schirmer, 2021). However, a model is only a replica of reality whose results are not precise and invariably have some degree of uncertainty (Anderson et al., 2015). In other words, the domination of uncertainties due to the lack of sufficient information and observation in the case study is inevitable, and therefore practical hydrogeology relies heavily on uncertainty estimation (Ramgraber & Schirmer, 2021). Management decisions and policies may suffer negative consequences due to the presence of uncertainty (Sikdar, 2019).

The main sources of uncertainty can be classified into three categories: a) parametric uncertainty, b) forcing uncertainty, and c) conceptual uncertainty. Parametric uncertainty arises from the lack or insufficiency of field data, which leads to uncertainty in the values assigned to model parameters. Forcing uncertainty refers to uncertainties related to external factors or inputs that force the system, such as unknown boundary conditions. Conceptual uncertainty arises from inadequate model structures, where the underlying conceptual framework may not fully capture the complexity of the system being studied (Ramgraber & Schirmer, 2021).

The modeling teams' interpretations and hypotheses of the GS can lead to different conceptualizations of the model and emphasized unquantifiable uncertainties such as the system structure and boundary conditions (Van Der Sluijs et al., 2005), which can be addressed through validation testing for comparison between the model results and the independent field observations (Højberg & Refsgaard, 2005). Despite its widespread use, this approach can only be used to evaluate model output variables for which equivalent field data are readily available. When extrapolatory predictions are made using models outside the bounds of the range of the currently available field data, this constraint becomes especially important (Højberg & Refsgaard, 2005).

Alternative approaches include an attempt to couple quantitative and qualitative (Van Der Sluijs et al., 2005), and utilization of multi-model approaches (Enemark et al., 2019). The adoption of a multi-model method, also referred to as multiple conceptual models, enables the explicit consideration of structural uncertainties (Højberg & Refsgaard, 2005). One drawback of this approach is that the probabilities associated with each scenario of the conceptual models are often unknown. Consequently, it becomes challenging to ascertain whether the multiple conceptual models adequately cover the entire range of plausible models (Højberg & Refsgaard, 2005).

Groundwater flow and transport processes can be studied using one of two main approaches: deterministic or stochastic. The deterministic approach involves creating a simulation model based on a thorough understanding of aquifer processes, while the stochastic approach accounts for uncertainties arising from limited knowledge of aquifer systems (Theodossiou et al., 2005). Stochastic modeling can address quantitative uncertainties resulting from the input parameters by using probability distributions to consider uncertainties in input values and the uncertainties in the outputs can be displayed using histograms or similar instead of point values (Anderson et al., 2015). The accuracy of aquifer parameters is crucial for delineating WHPAs. Since an incorrect WHPA can endanger public health, extreme care must be taken when using aquifer parameters like hydraulic gradient, thickness, conductivity, and porosity for WHPA delineation, as demonstrated by the study on the Dolton aquifer in eastern South Dakota (Bhatt, 1993).

Monte Carlo Simulation (MCS) is a stochastic approach that involves generating multiple results to address parameter uncertainties. This technique utilizes a probability distribution for uncertain values and generates random samples within predefined limits based on a known distribution and iteration. The results of these random samplings can be represented using a histogram, providing a general overview of the variability in the outcomes. Furthermore, MCS can be used to create multiple capture zones surrounding a well. A capture zone refers to the area surrounding a well that includes water and pollutants, which will ultimately be extracted within a certain time frame (Theodossiou et al., 2005). By generating random values for the uncertain input variables, multiple capture zones can be simulated. These capture zones depict the potential areas that could be affected by water and pollutant extraction from the well.

Most of the parametric uncertainties can be addressed by the application of a numerical model, although it would be time-consuming to implement such a model. Additionally, in terms of boundaries, numerical models have significant limitations as the exploration of the uncertainties' extent or nature due to the interdependency between the grid discretization and the boundaries can be difficult (Ramgraber & Schirmer, 2021).

Figure 2-6 represents the available methods for the delineation of the WHPA concerning the availability of data and ease of each approach. It is worth mentioning that there are different stochastic models to address the uncertainties of the input parameters.

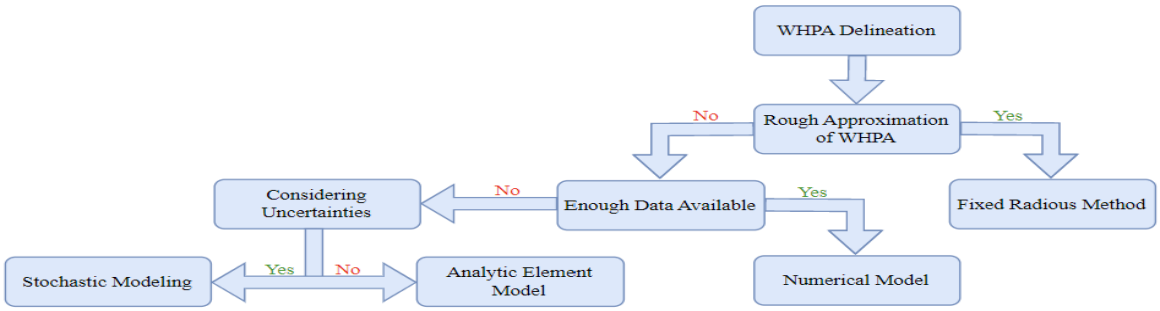

Figure 2-6. Methods for the delineation of WHPA, Extracted and modified from (Liu et al., 2019)

3

Case Study Site

This chapter gives a brief introduction to the case study area including the location, geology, aquifer type, hydrogeology, and the catchment area of the site. The description in this chapter is mainly based on the site description by the Geological Survey of Sweden, SGU (Lång & Lindh, 2016)

3.1 Håvesten aquifer

The Håvesten aquifer which is located approximately 2 km south of the Färgelanda municipality in a glaciofluvial deposit was selected as the study area (Figure 3-1). This aquifer stretches from north to south. The glaciofluvial deposit consists of layers of sand and gravel, and it is partially covered by fine-grained sediments consisting of clay. Hence, the groundwater recharge is limited, and the possible abstraction rate is estimated to be slightly above 5 l/s (class interval 5–25 l/s), which is in line with the estimated possible abstraction in the existing municipal groundwater sources.

Figure 3-2 shows the existing boreholes in the study area where the stratigraphy investigations have been done and the data is available (See Appendix A.2). Furthermore, the currently approved delineation zone as well as the catchment area can also be seen in this figure.

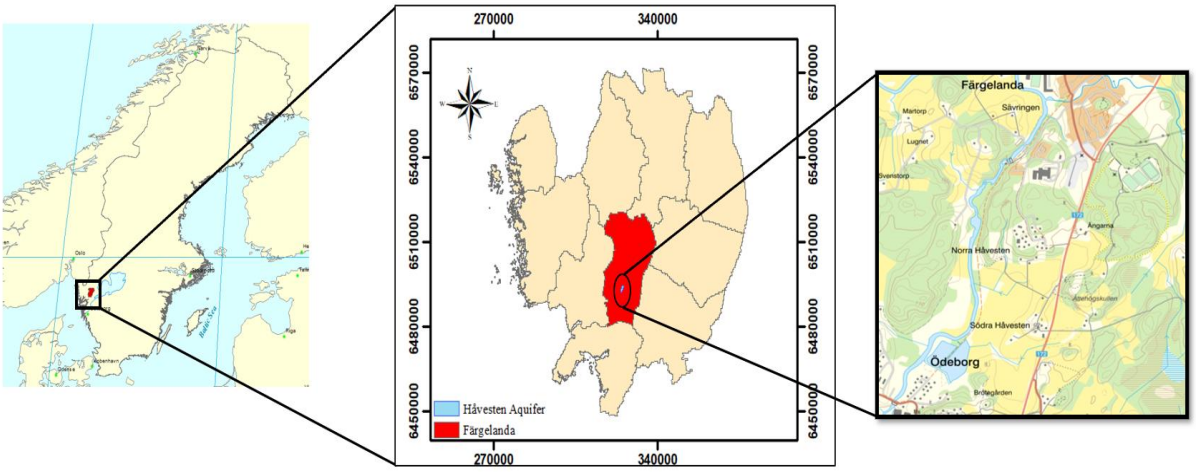

Figure 3-1. Location of the Håvesten aquifer (Extracted and modified from SLU University Library)

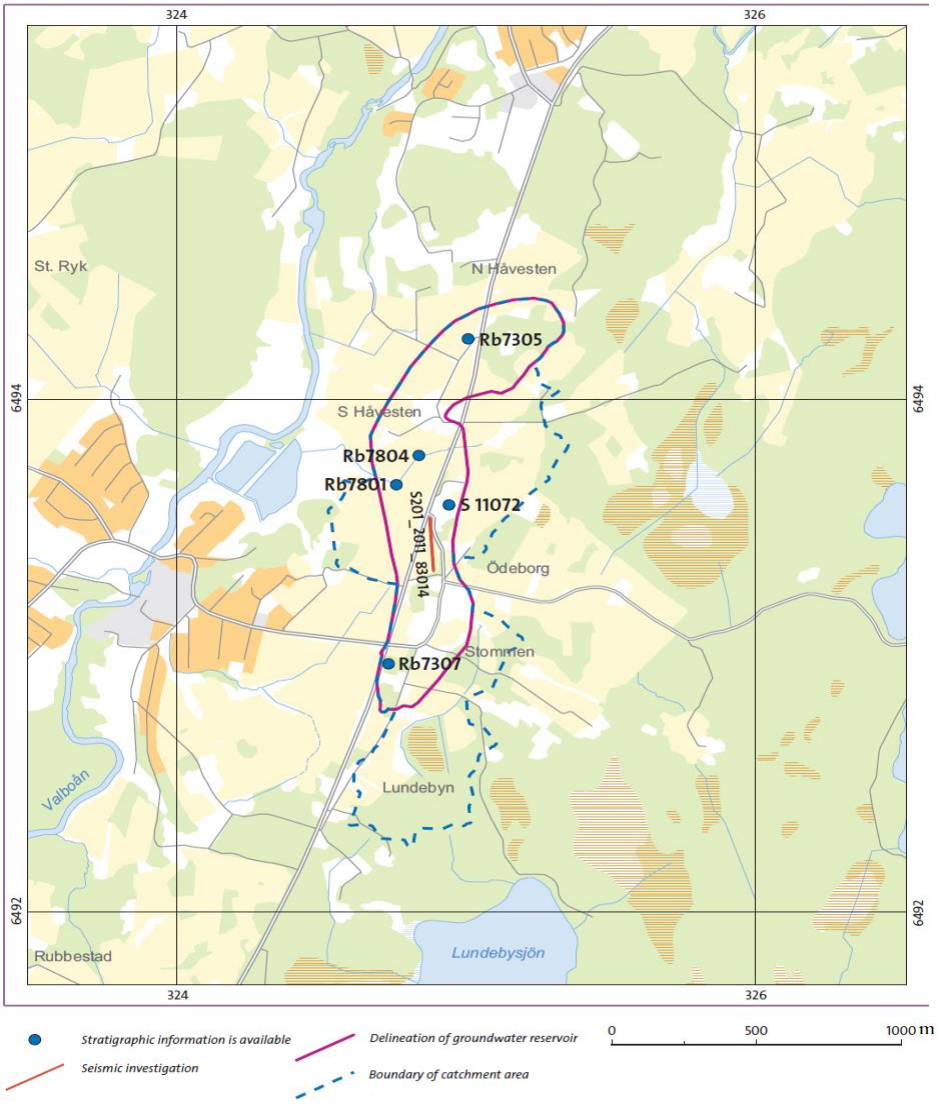

Figure 3-2. Location of the boreholes, the boundary of the catchment zone, and the current protection zone (Lång & Lindh, 2016)

3.2 Terrain and geological overview

The Håvesten groundwater source consists of a groundwater-carrying glaciofluvial deposit estimated to be roughly 1.5 km long and approximately 300 m wide. The aquifer consists of coarse-grained soil layers belonging to the glacial deposit and mainly consists of sand and gravel. Sand is considered to be the dominant fraction. The glacial deposit occurs within about half of the surface of the delineated aquifer, while the remaining part of it is overlaid by clay that is up to 10 m thick.

In the southern part of the aquifer, the glaciofluvial deposit continues and appears in the form of a ridge. Some smaller disused gravel pits are found in the glacial deposit. Outside the boundary of the aquifer, the soil layers close to the ground mostly consist of fine-grained sediments, mainly clay. This means that the delimitation of the extent of underlying coarse-grained layers, and thus also the extent of the aquifer, in these areas with fine-grained sediments is associated with uncertainty.

The topography varies greatly within the aquifer area. The highest parts are to be found in the north, where the ground level reaches 120 m above sea level, while the lowest is located in the clay-filled valleys with a level of approximately 85 m above sea level. The thickness of the soil layers varies between 15 and 25 m according to the refraction seismic survey (Figure 3-3). Drillings carried out show soil depths of up to 21 m. Rock outcrops occur adjacent to and in the surroundings of the aquifer, which reflects a significant variation in bedrock topography. Soil depth and the topography of the area can be seen in Figure 3-4.

The bedrock in the area is dominated by grey to red gneissic granite–granodiorite–tonalite. A minor occurrence of metamorphosed gneissic sandstone occurs within the area. The general strike of the rocks within the area is north-south. A couple of larger northeast-striking brittle deformation zones permeate the area.

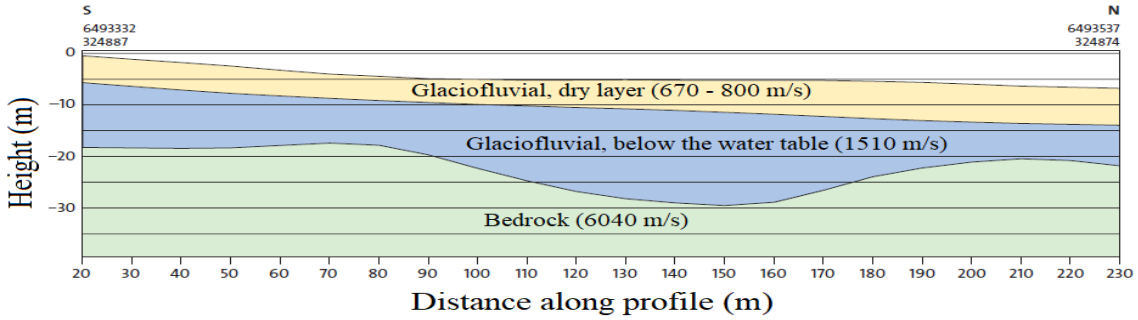

Figure 3-3. The seismic profile (Lång & Lindh, 2016)

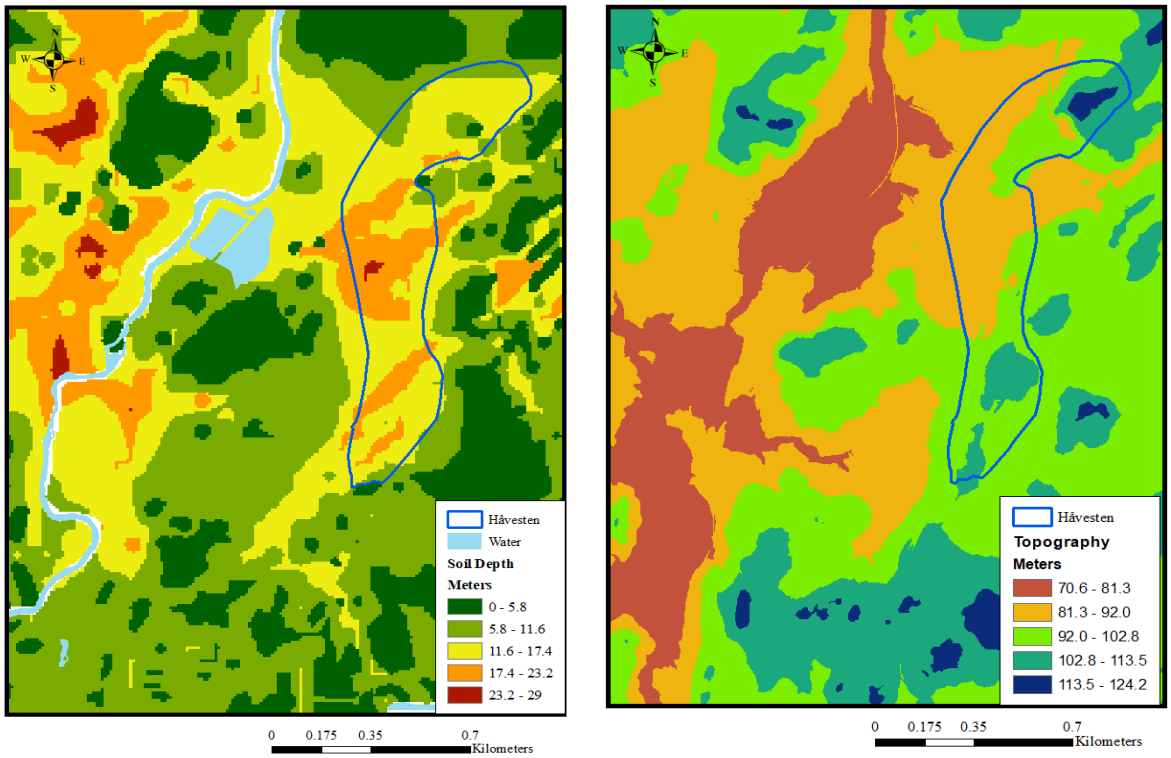

(a) (b)

Figure 3-4. Håvesten aquifer a) soil depth and b) topography (Extracted and modified from SLU University Library)

3.3 Aquifer type

As can be seen in Figure 3-5, clay covers most of the surface part of the study area, which means the Håvesten aquifer is confined in most places. After negotiations with an expert at SGU who has been studying the area (Lång, 2022), a better understanding of the aquifer type was achieved. Both observation wells S 11072 and Rb 7305 are located in the unconfined part of the aquifer, while the rest of the wells are situated in the confined part (see Figure 3-2). Moreover, the abstraction well is considered to be located in a confined condition. It is confirmed that small streams as well as other surface water features such as rivers and ponds in the area have no influence on the recharge and discharge conditions and do not interact with the aquifer.

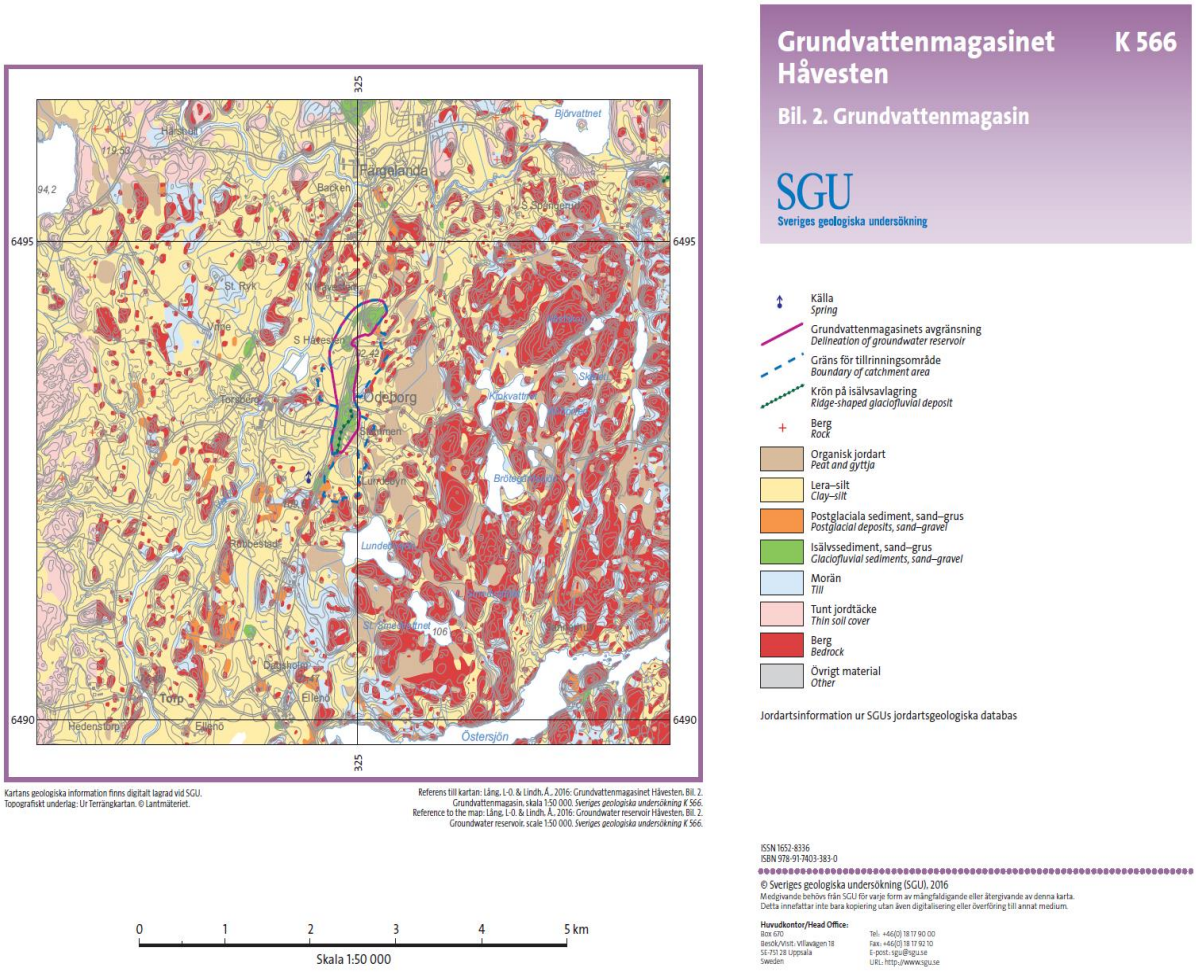

Figure 3-5. Geology of Håvesten aquifer (Lång & Lindh, 2016)

3.4 Hydrogeological overview

The variation in the rock and soil topography, the soil depth, and the layer sequences contribute to a heterogeneous structure of the aquifer. The thickness of the saturated zone also varies considerably between 7 and 17 m (Figure 3-3).

In connection with investigations at the Håvesten aquifer, it can be divided into two separated water sources: Håvesten I and Håvesten II, which are located in the north and south part of the main aquifer, respectively. The division of the aquifer is attributed to the presence of a finer-grained composition and less strength of the water-bearing layer in the area at Rb7804. The maximum capacity of 5 l/s that has been reported by SGU (Lång & Lindh, 2016), is based on the combined long-term withdrawal possibility of the entire aquifer, i.e., the sum of withdrawal from the reasonable number of wells with standard designs distributed in appropriate places within the aquifer. Based on the local water utility's investigations, Håvesten II has a withdrawal capacity of around 250 m^3/day (about 2.9 l/s), while this number is approximately 300 m^3/day (about 3.5 l/s) for Håvesten I, which has been used actively.

Groundwater recharge occurs in locations where the sand and gravel deposits are not covered by clay and silt layers. The direction of groundwater flow is generally towards the north, to be more specific, it can be said that the flow has a complicated regime and is most likely from the recharge area in the North-East direction. Both infiltration and recharge areas occur in the green part (See Figure 3-5). In the area at the water sources Håvesten I and II, it is stated that the drainage mainly takes place towards the west.

3.5 Catchment area and natural groundwater formation

The catchment area of the groundwater aquifer has been defined in a general way (Figure 3-6) and divided into the categories of primary and tertiary catchment areas (These concepts are described in Appendix A.3). A rough estimate of the natural groundwater formation provided to the aquifer from the primary catchment area is reported in (Table 3-1). No assessment of the size of the inflow from the tertiary catchment areas is reported, as there is no basis for such a calculation.

Table 3-1. Catchment areas, groundwater formation, and extraction possibilities (Lång & Lindh, 2016)

	Area (km^2)	Recharge (l/s)
Primary catchment area	0.25	4
Secondary catchment area	0	
Tertiary catchment area	0.67	Not assessed
Groundwater formation, coarse soil[1]	531 mm/year (16.8 l/s per km^2)	
Groundwater formation, moraine[1]	475 mm/year (15.0 l/s per km^2)	
Assessed maximum withdrawal possibility within the aquifer	5 – 10 l/s	

[1] The calculation of effective precipitation is based on climate data from the period 1962–2003 for the area in question. The uncertainty in the calculated value is significant.

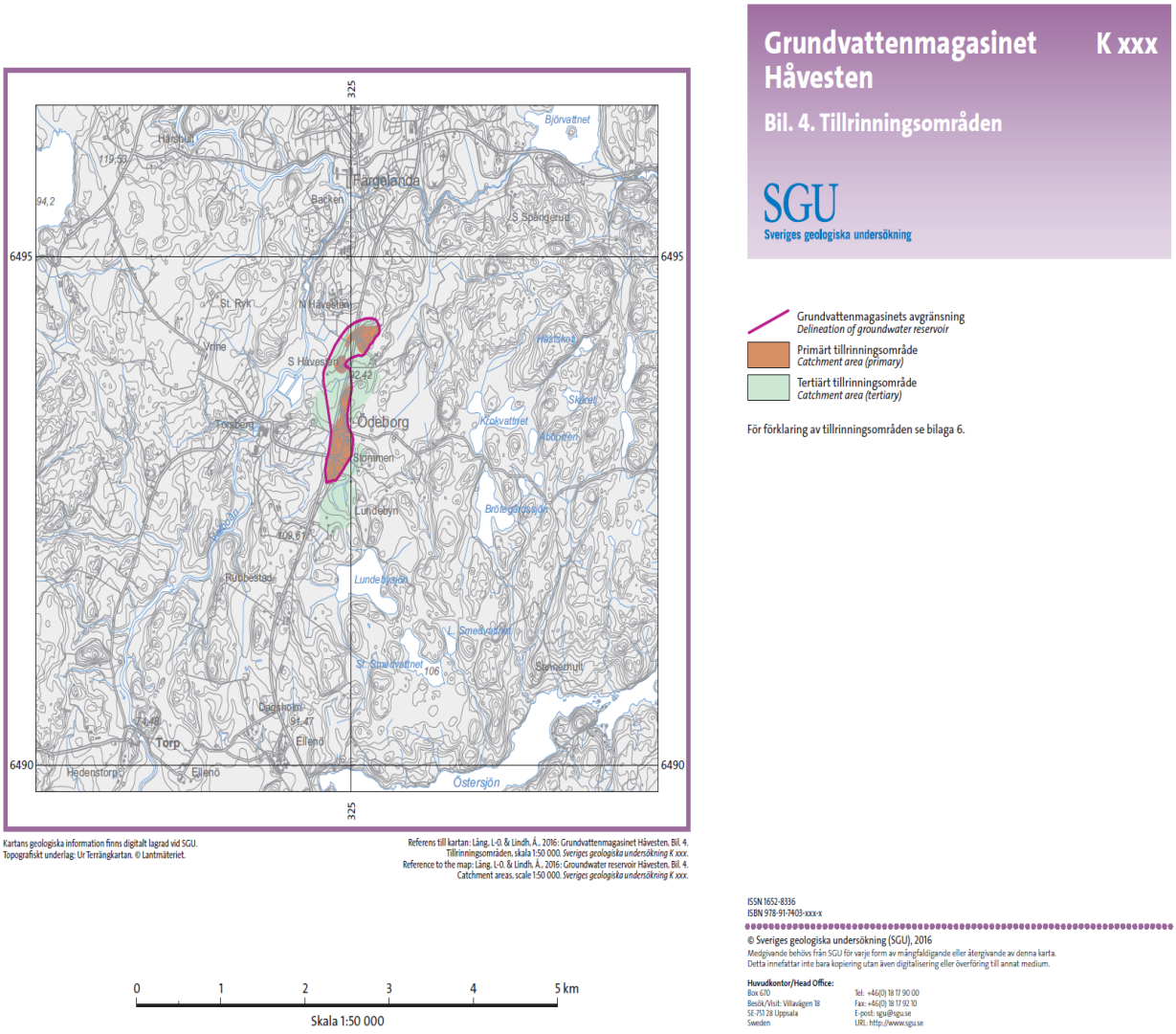

Figure 3-6. The primary and tertiary catchment area of the Håvesten aquifer (Lång & Lindh, 2016)

4

Methodology

This chapter gives an overview of the methods used for the delineation of the groundwater protection area at the Håvesten aquifer. Furthermore, it is crucial to emphasize that the approach presented in this study involves the successful implementation of MCS in AEM using TimML. Additionally, the necessary data for modeling, along with the corresponding code, are provided to support the implementation.

4.1 Overview

The research method used for this study is a mixture of groundwater flow modeling and particle tracking with consideration of uncertainties in input parameters. The WHPA is defined as the area where particles can move within groundwater flow when tracking their path lines in a backward direction. To model the aquifer, two methods are used: WhAEM 2000 (V.3.3.2) and TimML. Both methods use an analytic element model for the simulation of groundwater. However, for studying different scenarios such as the effect of recharge on the traces, the impact of pumping downstream on the final catchment area, and consideration of uncertainties, only the TimML which is an open-source model is considered. The working process which was used in this project is presented in Figure 4.1.

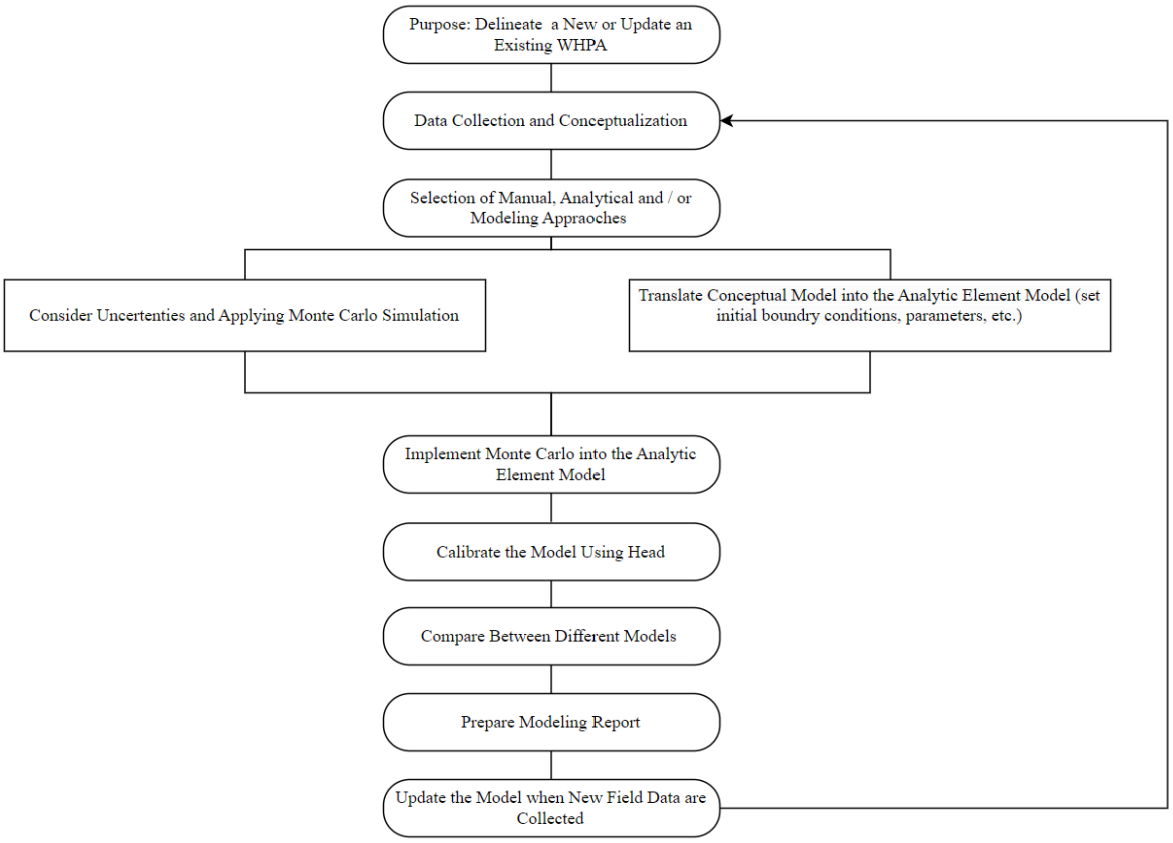

Figure 4-1. Workflow for groundwater modeling applied in this report

Based on the presented workflow, it is essential to emphasize that this study goes beyond merely comparing different software for modeling groundwater flow using an analytic element approach. The key steps involved in our work are as follows:

1. Implementation of Monte Carlo simulation (MCS) in TimML to address uncertainties in hydrogeological parameters.
2. Application of the developed model to the specific case study site.
3. Utilization of WhAEM as a comparative method for assessing the results.
4. Evaluation of the outcomes and examination of the practicality of our approach.

These additional steps ensure a comprehensive examination of the developed code and its applicability to real-world scenarios.

4.2 Applied models

4.2.1 Model setup in TimML

To set up the groundwater flow model in TimML, the following steps are required:

- Step 1: Integration of MCS in TimML
- Sep 2: Selecting the conceptual model
- Step 3: Assigning other properties of the model such as well location, type of flow, inhomogeneities, and impermeability based on the selected conceptual model,
- Step 4: Deciding on the number of iterations and the trace lines needed,
- Step 5: Assigning the aquifer's parameters to the model
- Step 6: Creating trace lines
- Step 7: Avoiding extreme values
- Step 8: Visualization by use of the graphs and collection of the results.

MCS has been seamlessly integrated into the TimML framework, enhancing the robustness of groundwater modeling by effectively addressing uncertainties and variability in the aquifer's parameters. The incorporation process begins by loading the output files of the MCS into TimML, as detailed in section 4.3. To enable sampling from the MCS-generated values for the parameter under consideration, a loop is implemented in the code. The number of iterations in this loop corresponds to the predefined value set by the user in step 4. For instance, for the primary and secondary zones in the Håvesten aquifer, 10 and 100 iterations are employed, respectively. This flexibility allows for tailored analysis based on the desired level of refinement. Within each iteration of the loop, random values for hydraulic conductivity, thickness, and porosity are selected from the MCS files that have been read by TimML. To achieve this, random.choice method in Python, which returns a random element from a provided non-empty list, is utilized. As a result, each run of the loop generates different models due to the varying parameter values, leading to a comprehensive exploration of the model's behavior.

Figure 4-2 illustrates the histograms showing the generated values obtained during an MCS process for the specific parameters under consideration. These data serve as the basis for sampling when executing MCS within the TimML framework. The MCS involves generating a total of 100,000 values employing a normal distribution.

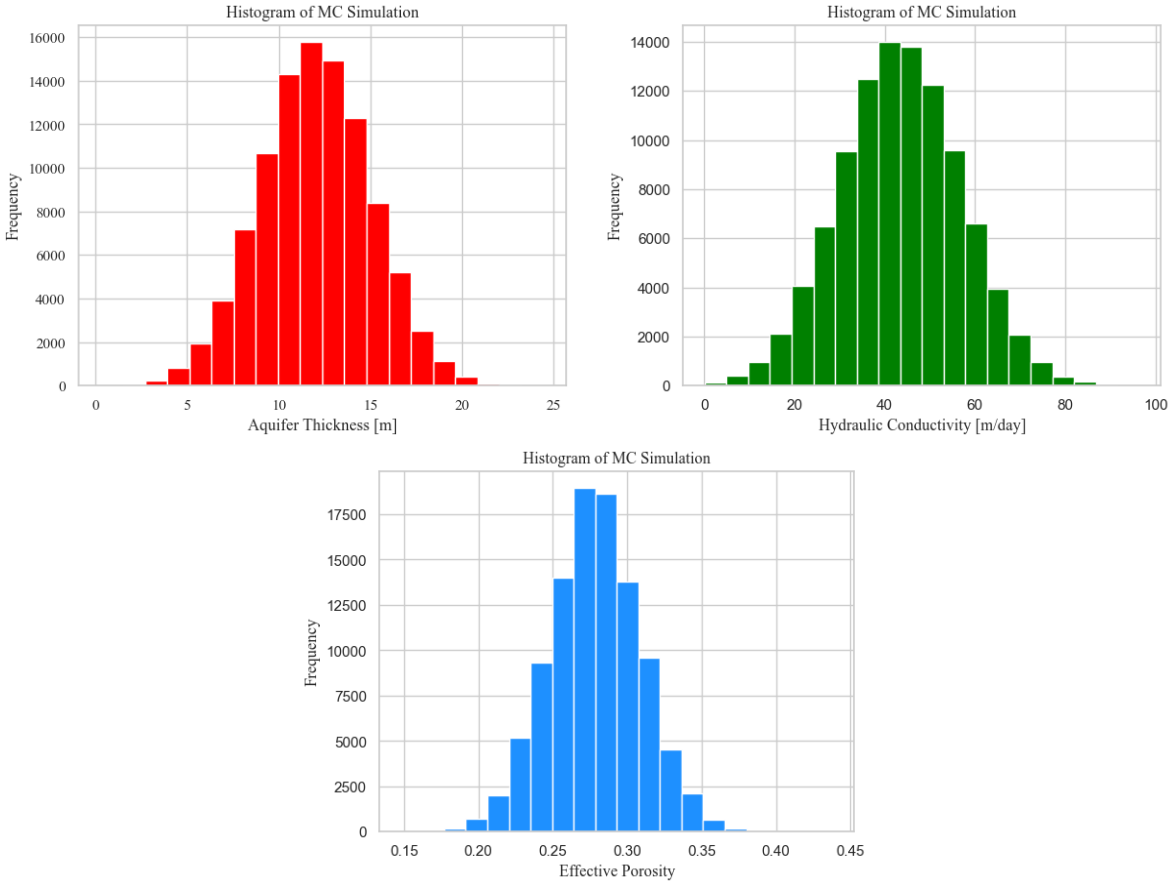

Figure 4-2. Generating normal samples by application of MCS

In the next step, the best conceptual model that can address all the boundaries in the study area should be modeled. This will be done by using the geological and hydrological maps of the area. To address uncertainties in the model and various assumptions in the development of conceptual models, eight scenarios are considered to simulate the aquifer, as can be seen in Figure 4-3. These strategies can be categorized into two main approaches: a) simulating only the Håvesten II confined aquifer, and b) modeling the entire Håvesten aquifer. These approaches are further explained in the next sections. After the selection of the conceptual model, the analytic elements which show different boundaries are implemented. It is worth mentioning that in both approaches, there is no need to model the streams and surface water features in the area, as they are assumed to not have any effect on the groundwater flow.

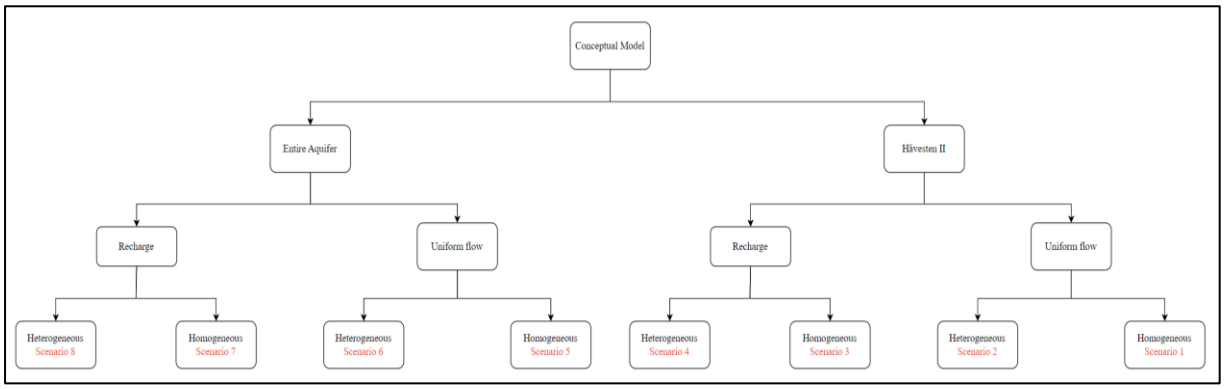

Figure 4-3. Conceptual models

The size of the study area, available computing power, and the desired level of accuracy directly influence the number of iterations required for the model in the fourth stage. The number of trace lines is also provided in this step. For the primary zone, the trace and iteration numbers are 20 and 10, respectively, to shorten computing time. However, the model then is run by applying 100 iterations to have more accurate results for the secondary zone.

In the subsequent step, after assigning the aquifer's parameters to the model, the data needs to be plotted on a graph to assess the correspondence between the model's predictions and the actual flow situation. The time of travel (TOT) is considered for different protection zones as follows:

- Primary zone = 100 days
- Secondary zone = 365 days (i.e., 1 year)
- Tertiary zone = the entire catchment

Thus, TOT values of 100 days and 1 year are assigned to calculate the primary and secondary protection zones, respectively.

To visualize the outcomes, the focus is on removing extreme values as a strategy. The process begins with solving the TimML model and storing the resulting trace line data. Subsequently, the dataset undergoes a filtering step where the top 10% of outputs, corresponding to the most extreme values, are removed from consideration. This removal effectively eliminates the outliers from the dataset and allows the consideration of uncertainties while ensuring that the highest 10% of values are not included. In other words, this approach defines the zone as the 90th percentile.

Finally, the trace paths are plotted on top of the Google map of the area to give the user a better understanding of the location of the potential contaminations which can enter the pumping well and result in the pollution of the underground drinking water resources of Håvesten aquifer. The code for this approach is provided in Appendix A.4.

4.2.1.1 First approach: modeling Håvesten II confined aquifer

This approach focuses solely on modeling the Håvesten II, which is a confined aquifer. To model the groundwater flow in this area, two strategies can be considered: a simplified approach using uniform flow or a more realistic model incorporating assigned recharge. In the

case of the latter, the recharge should just be assigned to the primary catchment area, as depicted in Figure 3-6.

The justification for applying uniform flow lies in the fact that the previous chapter established that the Håvesten aquifer is predominantly confined, meaning that the interaction between groundwater and surface water is negligible. Additionally, the impermeable clay covering the area makes it highly unlikely for recharge to penetrate the aquifer. Consequently, there is no need to model surface water features such as rivers, lakes, and streams. By using uniform flow, a suitable model can be generated (Badv & Deriszadeh, 2005). The TimML uniform flow is defined by hydraulic gradient and flow direction. These two characteristics are calculated using the three-point method (see section 4.4.5) and then incorporated into the model.

As it was mentioned previously the delimitation of the aquifer extent is associated with uncertainties. Therefore, either the entire study area can be assumed to be homogeneous with the same hydraulic conductivity and effective porosity or the aquifer can be surrounded by an impermeable wall formed by clay, where the K value is assumed to be equal to zero. In case of homogeneity, the next step is to simulate the rock outcrops which also behave the same as impermeable features. However, in a heterogeneous case, the recharge areas should be modeled. Next, the pumping well is modeled by entering its location and discharge. As mentioned in the case study chapter, Håvesten II has a discharge of 250 m3/day.

4.2.1.2 Second approach: modeling the entire Håvesten aquifer

In this approach, both the confined and unconfined portions of the Håvesten aquifer are considered, and a conceptual model akin to that used in WhAEM is adopted. However, an additional element is introduced by simulating a simplified version using uniform flow. It should be acknowledged that the behavior of the unconfined aquifer with uniform flow cannot be realistically represented. Nevertheless, this strategy is employed solely for comparison.

When delineating the WHPA, it is essential to take into account not only the individual protection zones associated with each pumping well but also the areas of overlap between these zones. Additionally, it is important to consider the formation of an overall zone that encompasses the combined WHPAs of all the pumping wells. By considering the overlapping zones and the collective area of the WHPAs, a more comprehensive understanding of the overall protection coverage can be obtained. In the study area, both the WHPA of individual wells and the overall protection coverage are calculated.

4.2.2 Model setup in WhAEM

To simulate the aquifer and estimate the WHPA using WhAEM software, the following input data are required: hydraulic conductivity, aquifer characteristics namely the thickness and the base elevation of the aquifer, porosity, and the pumping rates of the currently operating wells (Kraemer et al., 2000). Including in the additional model parameters is inhomogeneity where the hydraulic conductivity might vary dramatically, or in the case of the recharge area or bedrock outcropping.

The steps that are needed to model the groundwater in WhAEM2000 are as follows:

- Step 1: Loading the base map of the study area into the software
- Step 2: Assigning the aquifer properties and considering the geology of the area

- Step 3: Creation of analytic elements such as areal sinks and line doublets
- Step 4: Setting the contouring properties
- Step 5: Testing the conceptual model
- Step 6: Solve the model to see the head contours
- Step 7: Assigning the pumping rate and radius to the pumping center
- Step 8: Plotting particle trace lines
- Step 9: Draw the WHPA

To initiate the modeling process, three base maps are loaded into the software. These maps, obtained from the SLU website (SLU University Library, n.d.), provide information on the location of bedrock, the delineation of groundwater, and the recharge areas. Subsequently, the properties of the aquifer are incorporated into the model by assigning the average values of key parameters, including hydraulic conductivity, thickness, and porosity. It is worth noting that isochrone calculations, regardless of whether the ambient flow is considered, rely on average aquifer properties (Kraemer et al., 2000).

In the third step, well elements are incorporated into the confined and unconfined aquifers at the positions of the pumping wells. However, the exact location of the Håvesten I well is unknown. Therefore, for the unconfined aquifer, it is assumed that the pumping well is positioned at the centroid of the observation wells drilled in the Håvesten I.

To address both protruding bedrock and groundwater delineation, the horizontal barrier element is employed. Although incorporating additional details into the model can enhance accuracy, it may also prolong the computational time. Therefore, the modeling process proceeds without explicitly considering the presence of bedrock outside the groundwater delineation zone. Recharge areas are represented as inhomogeneities within the aquifer, characterized by the same hydraulic conductivity and porosity values. Moreover, the recharge value, as indicated in Table 3-1 is determined to be ($\frac{531}{1000\times365} = 1.45 \times 10^{-3}\ m/day$).

To establish the contour properties, a minimum contour elevation of 70.6 m, a maximum elevation of 124.2 m, and a contour interval of 1 m are considered. Additionally, an iteration number of 2 is incorporated into the model. This helps to refine the model and improve its accuracy by iteratively adjusting the parameters and fine-tuning the predictions. By progressively updating the estimated values based on the observed data, the software iteratively improves the representation of the aquifer's behavior and increases the reliability of the modeling results.

One possible approach for testing the implemented conceptual model is by introducing test points to the WhAEM model. These test points represent locations where the head or elevation is known, such as observation wells or the intersection of surface water and a contour line. The discrepancy between the model and observed heads can be recorded at these test points (Kraemer et al., 2000). In this project, the model is tested using observation wells with known heads located in Håvesten II. For tracing particles during the definition of the capture zone, the pumping center's radius will serve as the starting point. Since a small radius could compromise the particle's precision, a radius of 1 m is considered.

The resolution of the capture zone is determined by the number of trace lines, which in this case is set to 20. Assuming a fully penetrating well, the user has the option to set the initial altitude of the trace lines. It is important to note that this elevation should be above the base

elevation of the aquifer and below the water table (Kraemer et al., 2000). In this study, the trace lines are assumed to start 5 m above the aquifer's basic elevation, i.e., at an altitude of 77.63 m.a.s.l. For analyzing both the primary and secondary capture zones, a TOT of 100 and 365 days, respectively, is inputted into the model.

Finally, the delineation of the WHPA necessitates a manual process wherein the particle trace lines are carefully outlined. The aim is to encompass all the lines connecting the contamination source to the pumping well. Moreover, a comparison can be made between the manually delineated WHPA and the simplified version, which is either derived from an arbitrary or calculated radius.

4.3 Monte Carlo Simulation (MCS)

To set up an MCS, which can analyze a system's behavior by the generation of a distribution for a parameter, the below steps are followed:

- Step 1: Identifying the variables that have a significant impact on the system, in this study, hydraulic conductivity, aquifer thickness, and total porosity are considered as the parameters with high influence.
- Step 2: Defining the type of distribution that is needed for the generation of values. The type of distribution for the K value is assessed using the method above, while for the other two remaining parameters, due to a lack of data, a normal distribution is assumed.
- Step 3: a set of values is generated using the Python built-in functions based on the type of distribution. It is important to note that these values are generated as a preliminary step for later sampling, and the process involves 100,000 iterations.
- Step 4: Running the simulation based on the input data, i.e., calculated mean value and the standard deviation.
- Step 5: Visualization of the results by application of graphs.
- Step 6: Collect the results as the output and use them in further analysis.

It is worth mentioning that validation of the output is also an important step to compare the results with real-world data to readjust the model in case of any unexpected behavior. However, due to a lack of information at the time of conducting this study, no emphasis is placed on this step (see Appendix A.5).

4.4 Input data

In this section, the required data for modeling the groundwater to define the WHPA is presented. It is important to highlight that uncertainties in some of the inputs are considered to enable MCS.

4.4.1 Hydraulic conductivity (*K*)

From a previous investigation in the studied area, data for one well was obtained. The available information includes the grain size distribution and the calculated hydraulic conductivity. Thus, the *K* values of this well, which can be seen in Table 4-1, are used as the representative of the entire area.

Table 4-1. Hydraulic conductivity in Rb 7801 (VIAK AB, 1978)

Depth (m)	d_{10} (mm)	d_{60} (mm)	d_{60} / d_{10}	K_i (x 10^{-3} m/s)
13.0 – 14.0	0.074	0.19	2.6	0.07
14.0 – 15.0	0.125	0.32	2.6	0.25
15.0 – 16.0	0.135	0.45	3.3	0.27
16.0 – 17.0	0.125	0.32	2.6	0.25
17.0 – 18.0	0.18	0.6	3.3	0.56
18.0 – 19.5	0.27	4.0	14.8	0.95
19.5 – 20.5	0.08	0.36	4.5	0.06
20.5 – 21.0	0.23	0.8	3.5	1.04
21.0 – 21.3	0.25	1.4	5.6	1.06

To generalize these values to the entire region, first, the dominant type of distribution should be identified. Since for hydraulic conductivity, either the normal or the log-normal distribution prevails, only the comparison between these two types of distribution is considered. Figure 4-4 demonstrates that the provided hydraulic conductivity data can be adequately fitted by both the normal and log-normal models. However, upon conducting a thorough analysis through the goodness of fit assessment (refer to Appendix A.6), it becomes apparent that the log-normal distribution exhibits a slightly superior fit. Nonetheless, to facilitate the calculation of essential statistical parameters such as UCLM 95 and establish a probability distribution for the mean value, a normal distribution is ultimately selected for its convenience.

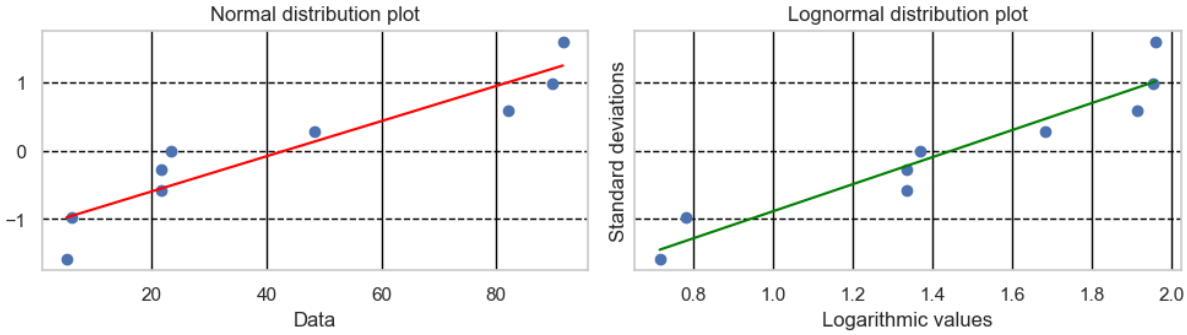

Average	43.30
Standard Deviation	35.72
UCLM 95	65.44
LCLM 95	21.15
Share > action target	79%

Median	28.16
Average	51.26
Standard Deviation	77.94
Chebyshev UCLM 95	156.54
Share > action target	72%

Figure 4-4. Finding the best fit for hydraulic conductivity by comparing the normal and log-normal distribution

In the subsequent phase, the 95% confidence interval of the sample mean is computed and employed to establish the uncertainty distribution utilized for the hydraulic conductivity during the execution of the MCS. The UCLM95 denotes the upper 95% confidence limit of the mean, while $\bar{x}$ is the sample mean.

4.4.2 Aquifer thickness (*H*)

The aquifer thickness data was retrieved from the seismic profile of the studied area provided by the SGU report (Lång & Lindh, 2016). As mentioned previously, this parameter can fluctuate along the aquifer from 7 to 17 m. The midpoint of the range is considered as the mean value which is equal to 12 m. The minimum and maximum values are used to define the 5th

and 95th percentile in the normal distribution used to model *H*. The thickness of the aquifer is determined relative to a base elevation, and the uncertainty in the base elevation does not affect the results. According to Figure 3-3, the bottom layer of the Håvesten aquifer is located 23 meters below the ground surface. By examining the topography map (Figure 3-4), it can be found that the average altitude of the ground surface in the case study is 95.63 m.a.s.l. Consequently, it can be deduced that the base elevation for the aquifer is 72.63 m.a.s.l.

4.4.3 Porosity

The most significant aquifers in Sweden are glaciofluvial sand and gravel deposits. The chosen site is also mainly covered by glaciofluvial deposits. For the study area, an assumed mean value of 27.81 and a range of 22.74 to 32.88 were derived based on Gupta & Ramanathan (2019). Similar to the aquifer thickness, porosity is modeled using a normal distribution, with the minimum and maximum values representing the 5th and 95th percentiles, respectively. is chosen for modeling the porosity. The average property values of the Håvesten aquifer are provided in Table 4-2, while Table 4-3 presents the essential statistical parameters required to generate an MCS for hydraulic conductivity, aquifer thickness, and porosity of the Håvesten aquifer.

Table 4-2. Properties of Håvesten aquifer

Type of aquifer	Aquifer thickness [H (m)]	Effective porosity [n (%)]	Hydraulic conductivity [K (m/day)]
Mostly confined	12	27.81	43.3

Table 4-3. Statistical parameters

Parameter	Mean	Standard deviation	LCLM95	UCLM95
Hydraulic conductivity [K (m/day)]	43.30	13.46	21.15	65.44
Aquifer thickness [H (m)]	12	3.04	7	17
Effective porosity [n_e]	0.2781	0.0308	0.3288	0.2274

4.4.4 Head observations

The heads of the observation wells were obtained from the local water utility responsible for the area and are presented in Table 4-4. To determine the groundwater level, measurements were recorded on two separate dates and labeled as groundwater level 1 and groundwater level 2 in the table. In the models, the head is the average value among the first and second measurements. Additionally, Figure 4-5 displays the location of the observation wells where the heads were measured.

Table 4-4. Values of head observations in (m.a.s.l)

Observation well	Aquifer	Ground level	Top of the well	Bottom of the well	Length of the well	Groundwater level 1	Groundwater level 2
Rb 7401	Håvesten I	91.128	91.784	-	-	83.264	83.684
Rb 7308	Håvesten I	84.714	86.118	65.348	20.77	83.468	83.818
Rb 7402	Håvesten I	92.549	93.649	78.689	14.96	83.529	83.889
Rb 7802	Håvesten II	91.51	92.547	87.177	5.37	89.127	89.227
Rb 7803	Håvesten II	93.554	95.454	75.754	19.7	89.184	89.334

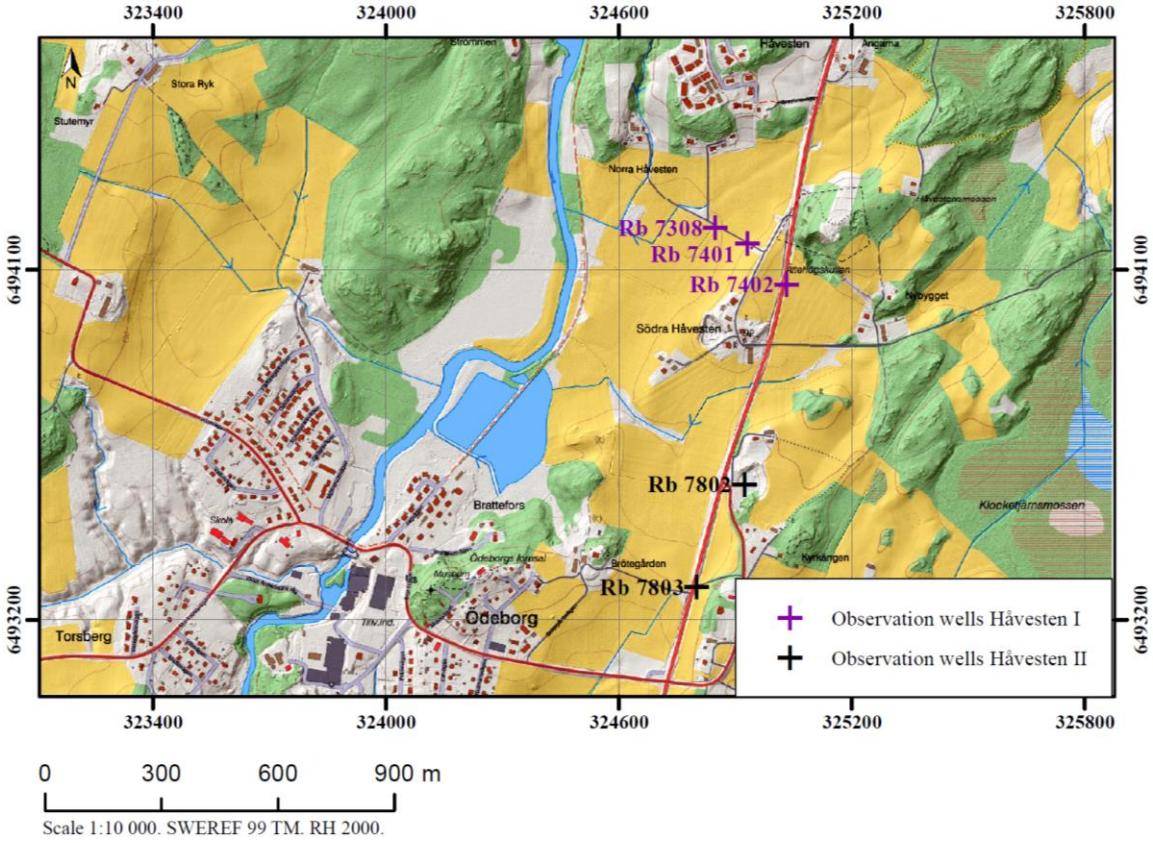

Figure 4-5. Geological placement of the wells in the area (source: Lantmäteriet)

4.4.5 Hydraulic gradient and direction of the flow

The hydraulic gradient (i) and the flow direction of the groundwater (θ) can be calculated by knowing: 1) the total head; 2) the geographic coordination; and 3) the inner distance in at least three wells that create a triangular configuration in an aquifer (Heath, 1983). In this approach which is called the "three-point method" the bias in the estimated parameters is reduced using the water level. The step of this approach is as follows (Badv & Deriszadeh, 2005; Heath, 1983; Kraemer et al., 2000):

a) Detect the observation well that has the intermediate water level
b) Compute the position between the observation wells with the highest and the lowest head where the head is equal to the head in the intermediate well.
c) Using a straight line, the intermediate well is connected to the point identified in step b. Along the drawn line, which represents a water-level contour segment, the total head is the same as the head in the intermediate well.
d) Through either the well with the highest head or the well with the lowest head, a line perpendicular to the contour of the water level is drawn which illustrates the direction of the flow.
e) The hydraulic gradient is defined as the ratio of the head difference to the distance between the well in step d and the contour.

Due to the limited number of head measurements available in Håvesten II, the method is implemented primarily based on data from Håvesten I. It is assumed that the flow in both aquifers follows a parallel pattern, thereby providing a reasonable approximation for the current

study. Utilizing the head measurements presented in Table 4-4, it is evident that Rb 7308 serves as the observation well exhibiting intermediate head values. The direction of the flow is indicated as 55.55° in Figure 4-6. Additionally, the hydraulic gradient can be determined as follows:

$$i = \frac{83.709 - 83.643}{6.49} = 0.01017 \qquad \text{Equation 4.1}$$

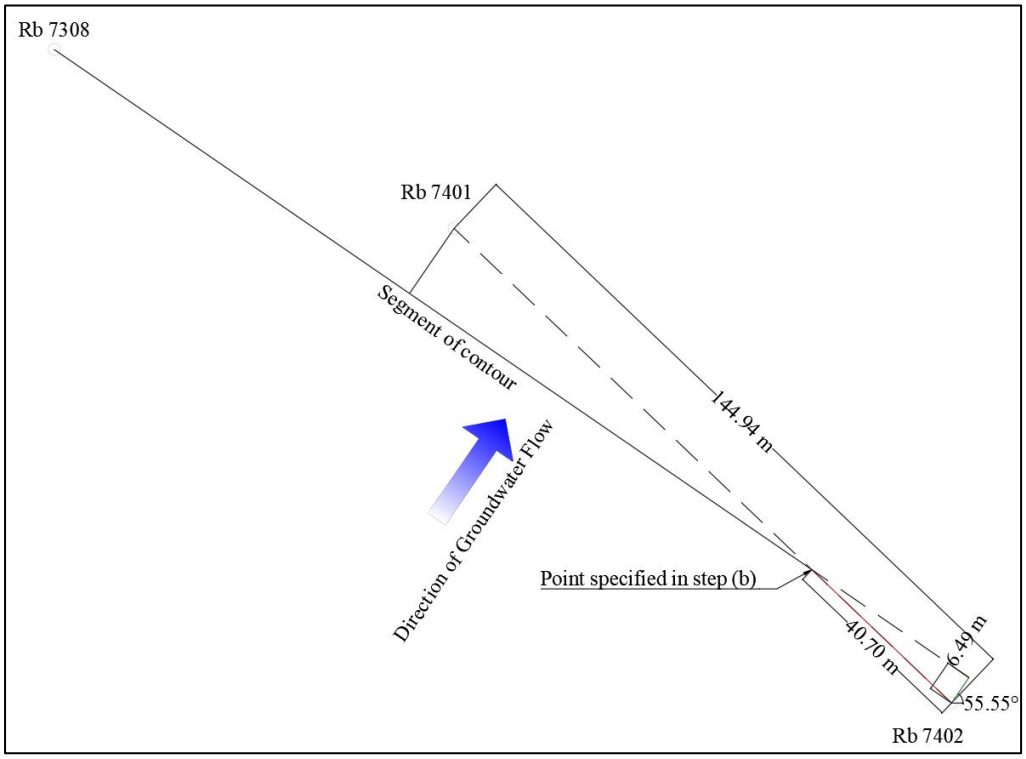

Figure 4-6. Three-point method for calculation of hydraulic gradient and flow direction

5

Results

This chapter aims to present the results of both TimML and WhAEM and gives a comparison between the delineation of the WHPA with and without the consideration of the uncertainties in the input parameters and conceptual models.

5.1 Model outcome

The subsequent sections present the results obtained from both the TimML and the WhAEM software. To facilitate a comprehensive comparison, all the results are consolidated within the comparison section and visualized in a single graph. This approach enables a more effective evaluation and examination of the outcomes.

5.1.1 TimML results

As it was mentioned in the previous chapter, 8 different scenarios are considered to investigate the effect of uncertainty in the conceptual model on groundwater behavior. These scenarios and their description can be seen in Table 5-1.

Table 5-1. Different conceptual models considered for modeling the aquifer

Scenario	Description					
	Modeling Håvesten II	Modeling the entire aquifer	Uniform flow	Recharge	Homogeneous	Heterogeneous
1	✓		✓		✓	
2	✓		✓			✓
3	✓			✓	✓	
4	✓			✓		✓
5		✓	✓		✓	
6		✓	✓			✓
7		✓		✓	✓	
8		✓		✓		✓

5.1.1.1 Head contours

The head contours for each implemented scenario are visually presented in Figure 5-1, with particular focus given to the head at the observation well Rb 7803, serving as the reference point. To provide a comprehensive analysis, trace lines are depicted based on running the model with a TOT of 1 year, using average values for the aquifer hydrogeological properties. To differentiate between the scenarios, the trace lines corresponding to Håvesten II are distinguished by their blue color. These lines allow for a clear visualization of the flow patterns and behavior associated with these specific scenarios. On the other hand, in situations where the entire aquifer is modeled, the particle trace lines for Håvesten I are highlighted in orange, enabling a distinct representation of the flow dynamics within these configurations.

Additionally, two specific scenarios, denoted as scenario number 8, are presented for further analysis. In the first scenario, the existence of rock outcrops within the recharge area is disregarded, assuming a homogeneous distribution of the recharge area. Conversely, the second scenario accounts for the presence of these outcrops, resulting in a reduction in the overall area available for recharge.

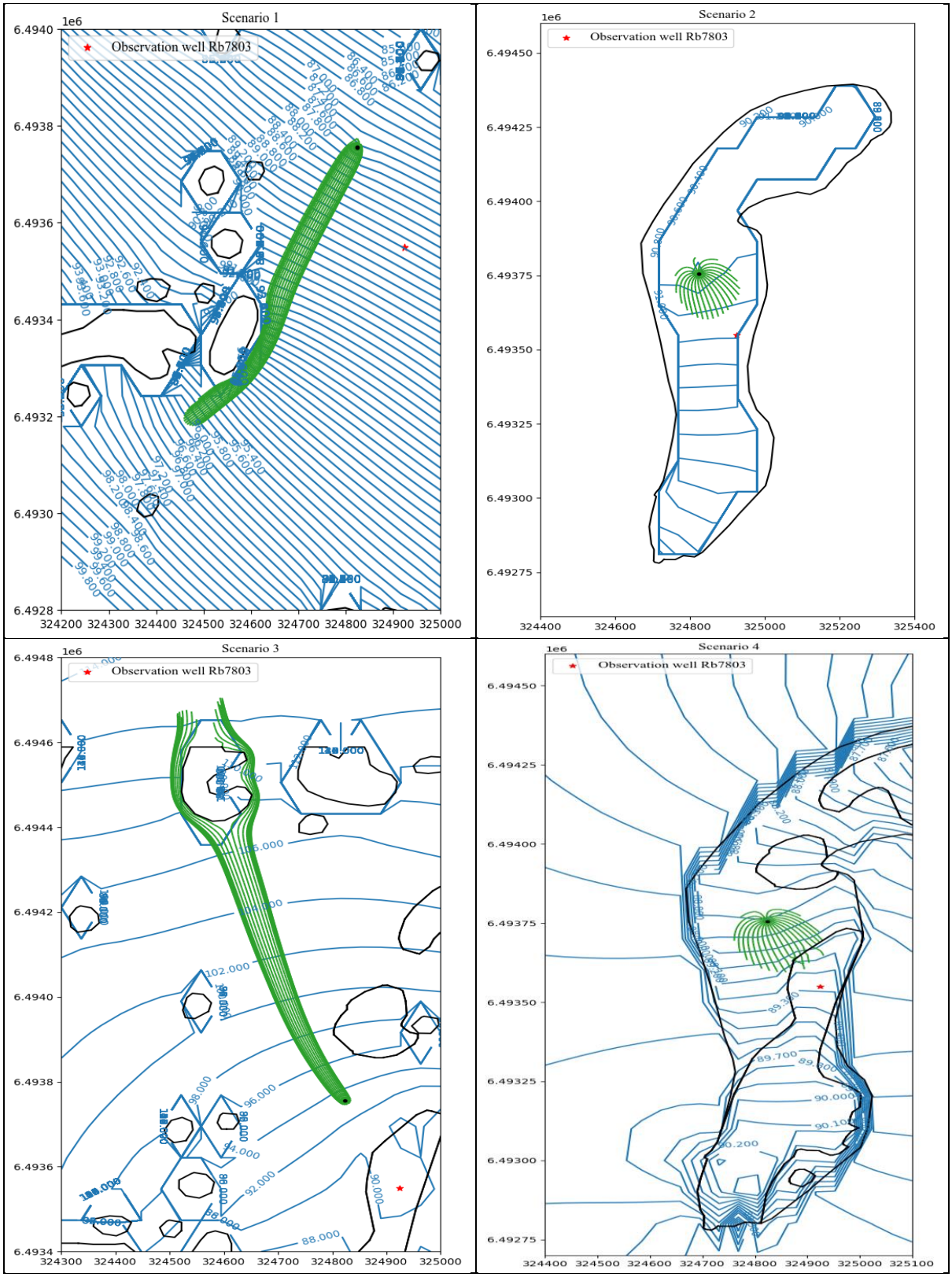
Scenario 1
Observation well Rb7803
1e6
Scenario 2
Observation well Rb7803
1e6
Scenario 3
Observation well Rb7803
1e6
Scenario 4
Observation well Rb7803
1e6

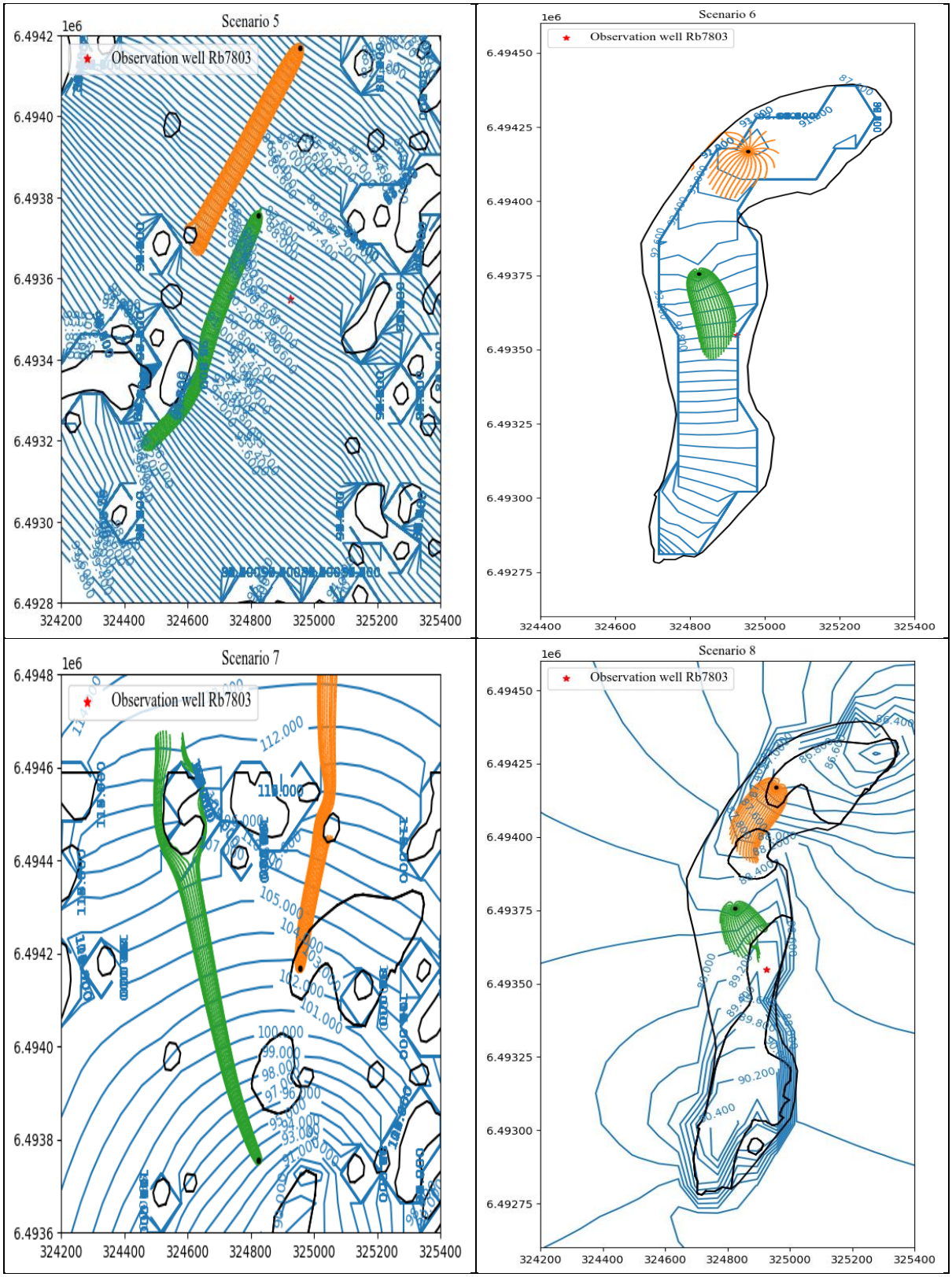
Scenario 5
Observation well Rb7803
Scenario 6
Observation well Rb7803
Scenario 7
Observation well Rb7803
Scenario 8
Observation well Rb7803

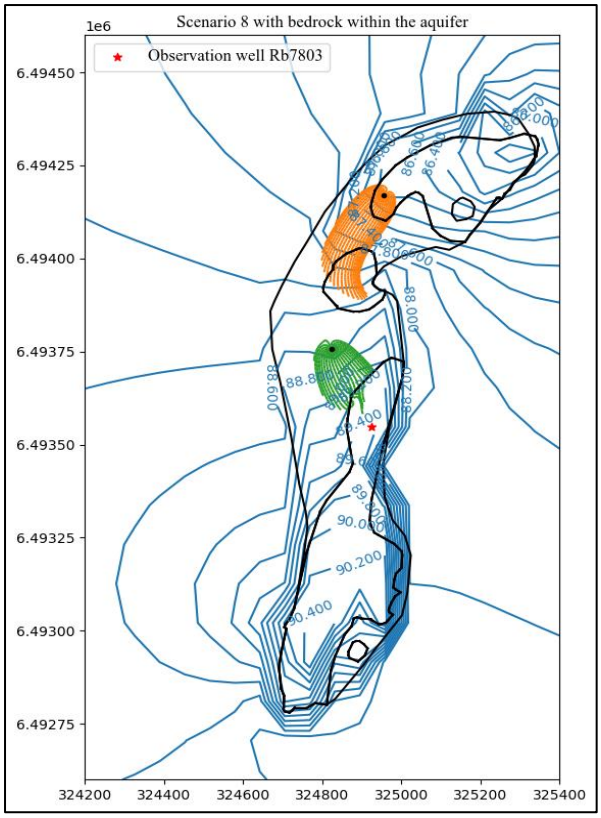

Figure 5-1. TimML head contours in different scenarios

5.1.1.2 WHPAs

The WHPA represents a curve encompassing all trace lines, as shown in Figure 5-2 and Figure 5-3, for a TOT of 100 days and 1 year, respectively. These figures solely consider abstraction from Håvesten II, as denoted by scenarios 1 to 4. However, scenario 3 has been excluded from the primary scenarios due to its failure to meet the required contour head and its west-north-to-south flow direction. The remaining scenarios demonstrate their adherence to both the contour head and the flow direction highlighted in the case study chapter. Furthermore, it is worth mentioning that the delineation of the groundwater, as stated by the SGU (Lång & Lindh, 2016), is depicted by a black dashed line in these figures.

Figure 5-4 displays the separate WHPAs for Håvesten I and II, with a TOT of 1 year. In contrast, Figure 5-5 represents the WHPAs for the entire aquifer, combining the protection zones for both Håvesten I and II under the same conceptual model scenario. These figures encompass scenarios 5 to 8, except scenario 7 which is excluded due to the observed north-to-south flow direction that is based on the depicted contour lines and contradicts the expected south-to-north flow pattern. Figure 5-6 illustrates the primary protection zones for the entire aquifer with a TOT of 100 days. It is important to note that the protected areas are defined by considering only the trace lines of Håvesten II wells, as combining the primary WHPAs for Håvesten I and II would be irrelevant and misleading.

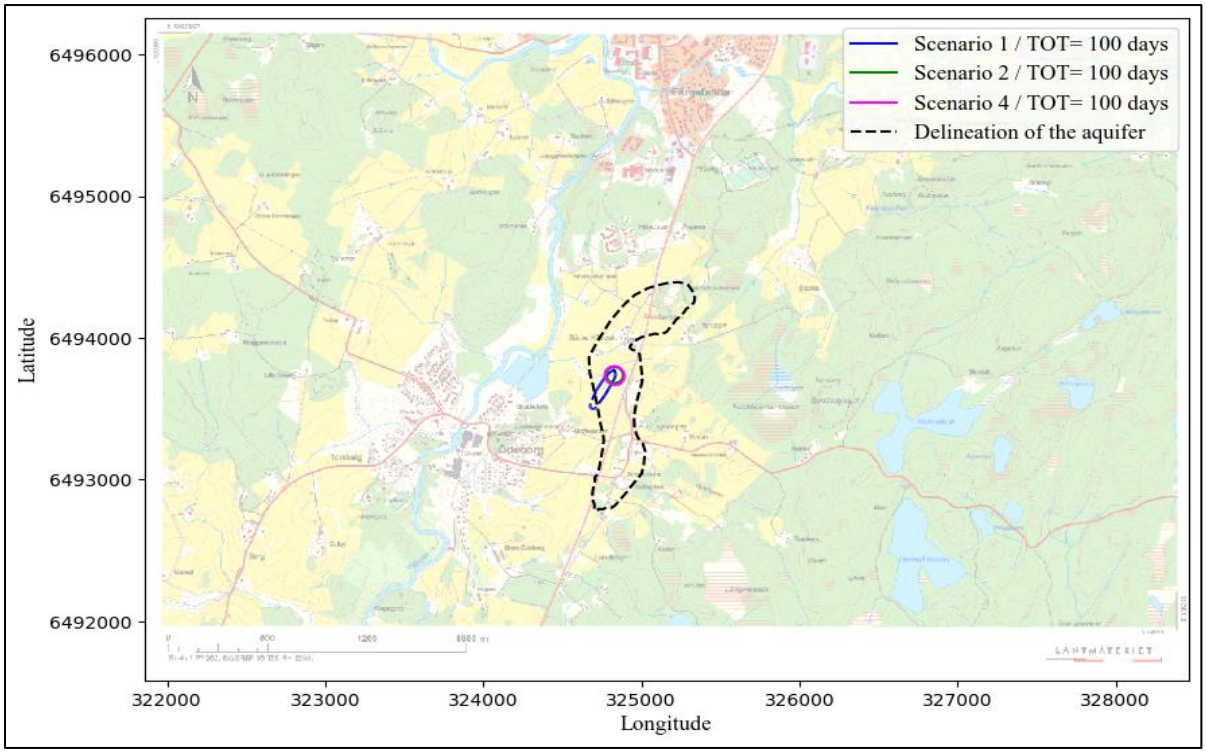

Figure 5-2. Primary WHPAs of Håvesten II

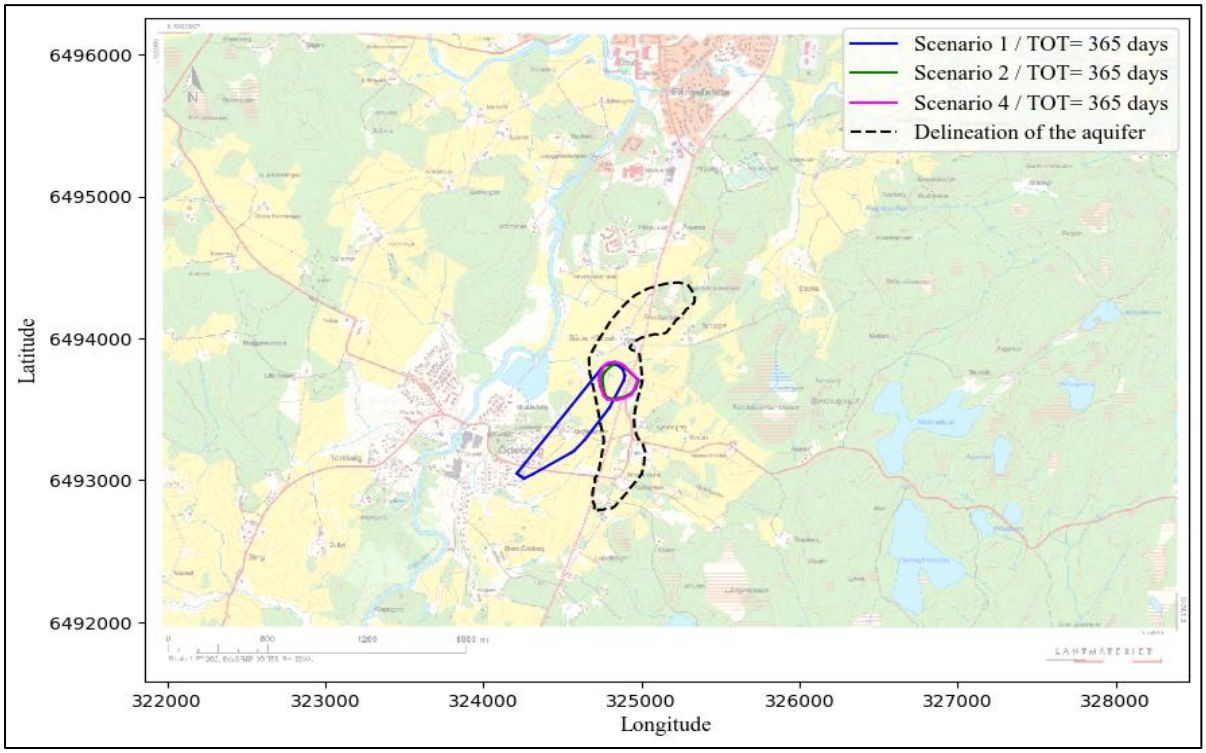

Figure 5-3. Secondary WHPAs of Håvesten II

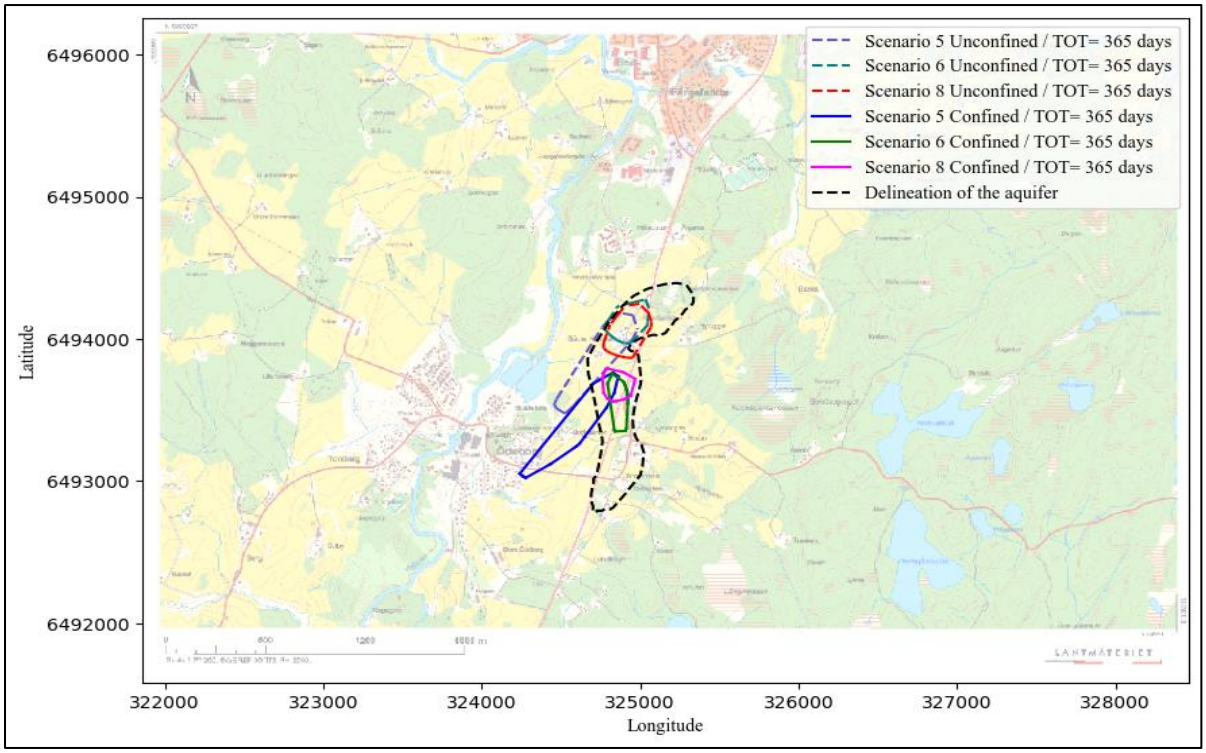

Figure 5-4. Secondary WHPA of Håvesten I and II

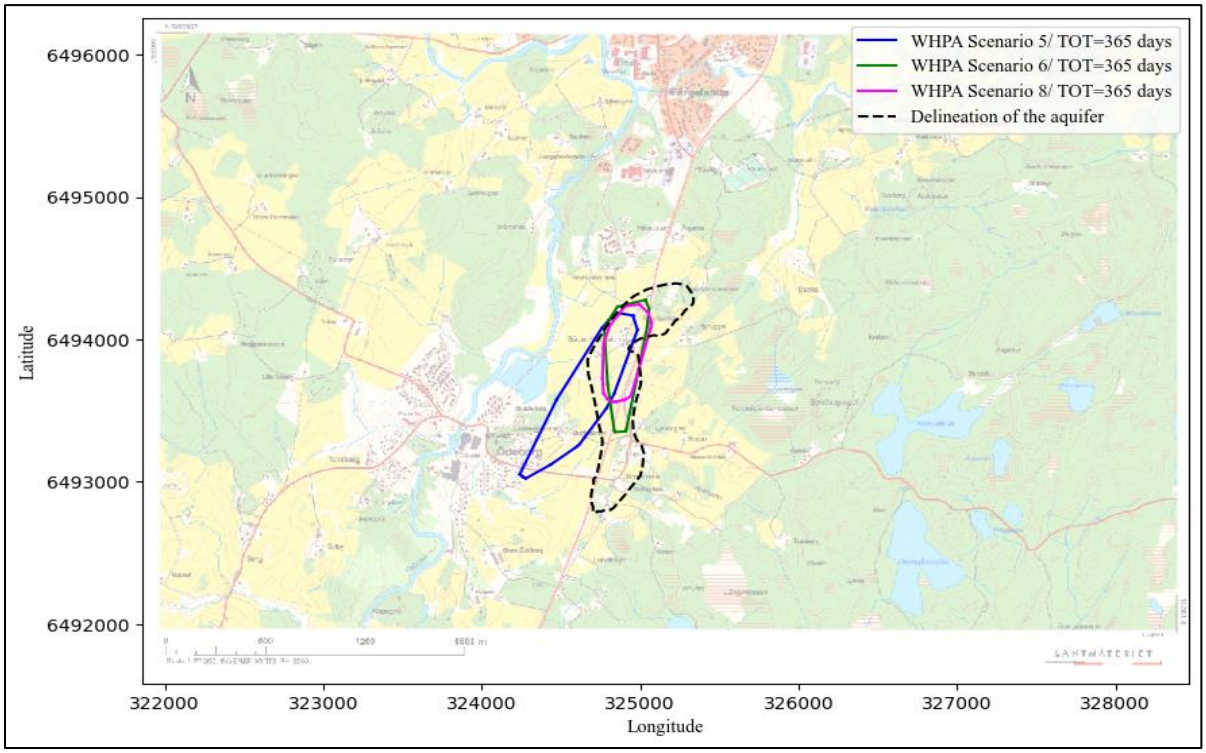

Figure 5-5. Secondary WHPAs of the entire aquifer for Scenarios 5 to 8

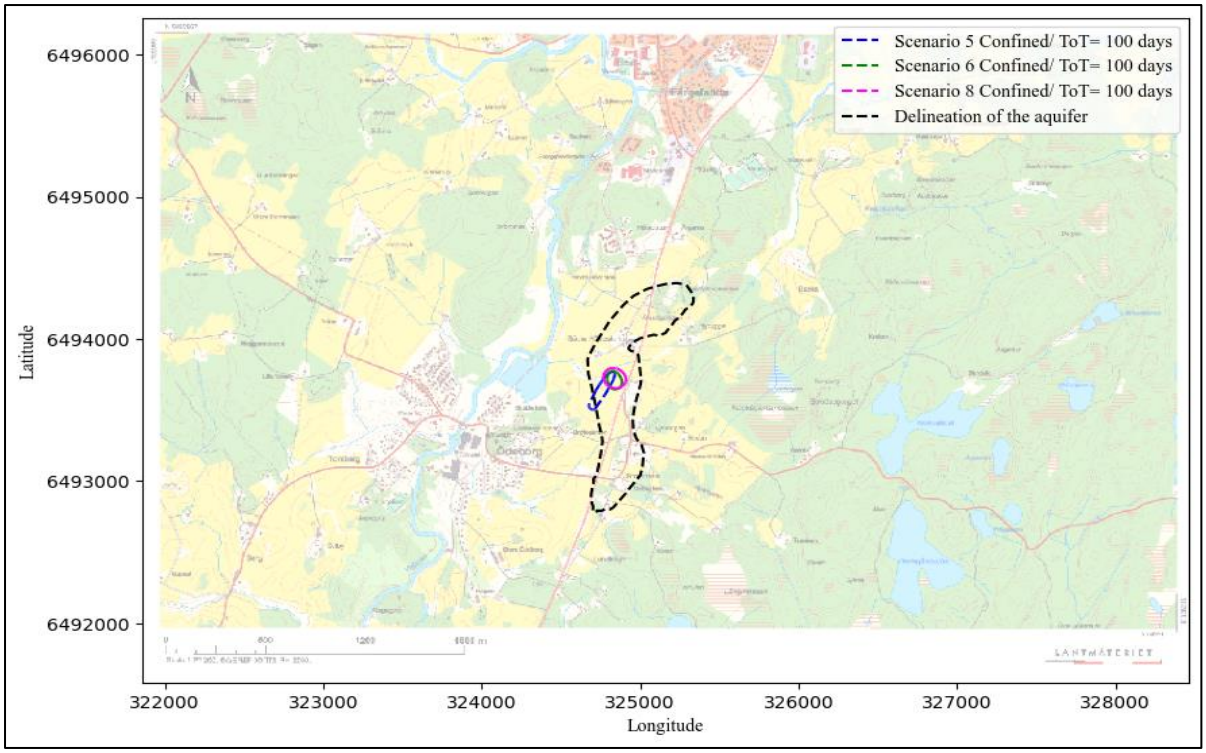

Figure 5-6. Primary WHPAs for Scenarios 5 to 8

The area that should be protected based on each scenario is collected in Table 5-2. The scenarios which fail to fulfill the requirements are excluded from the table.

Table 5-2. Area of primary and Secondary WHPA in different scenarios

ID	Primary WHPA (m^2)	Secondary WHPA (m^2)	Secondary 90% WHPA (m^2)
Scenario 1	15,909	174,477	168,697
Scenario 2	9,773	75,431	40,640
Scenario 4	12,847	60,515	48,176
Scenario 5 – Håvesten II	16,326	143,170	128,032
Scenario 5 - combined	-	323,167	303,268
Scenario 6 - Håvesten II	9,352	77,584	37,639
Scenario 6 - combined	-	289,115	169,799
Scenario 8 - Håvesten II	15,676	48,343	35,532
Scenario 8 - combined	-	166,650	147,696
Scenario 8 -with rock-Håvesten II	15,235	50,452	38,732
Scenario 8 – with rock-combined	-	162,332	151,423

5.1.2 WhAEM result

The result of WhAEM software is illustrated in Figure 5-7, establishing the necessity for calibration of the model. The forthcoming calibration process entails adjusting the hydraulic parameters, thereby ensuring enhanced accuracy and reliability. In Figure 5-4, the particle tracking lines of Håvesten I and II are represented by the red and blue lines, respectively. Furthermore, the curves in the graph illustrate inhomogeneities within the study area. The red curve indicates the delineation of groundwater, the green curves represent the recharge areas,

and the yellow curve represents the rock outcrop. Additionally, the red triangles on the graph indicate the locations of test points where the hydraulic head is known.

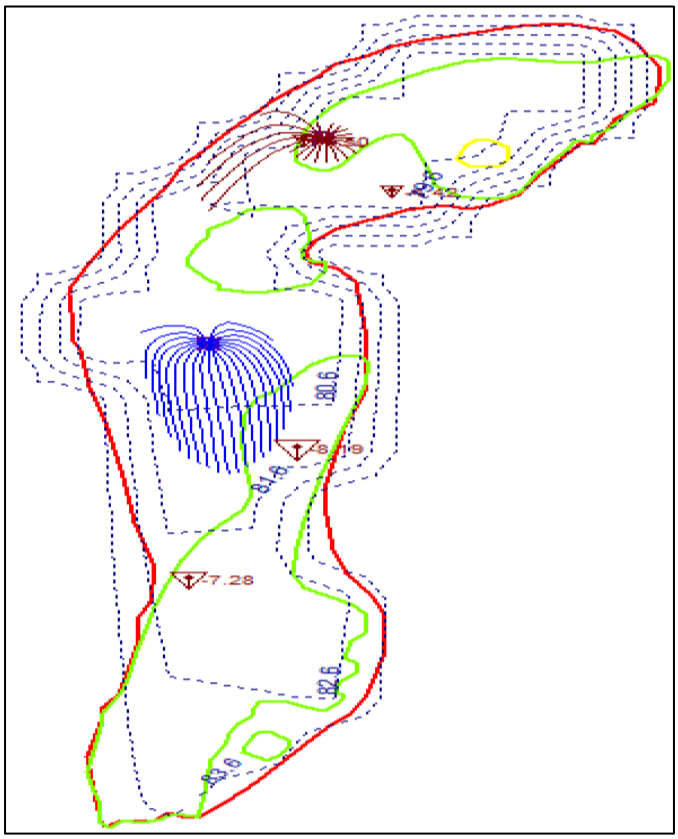

Figure 5-7. Traced particles in WhAEM

Therefore, to achieve an accurate representation of the actual conditions, it is imperative to calibrate the model. This calibration process involves the incorporation of test points into the model, enabling a comparative analysis of the measured and modeled heads through WhAEM. By adjusting the input parameters, the model undergoes refinement until reaching an optimal state, as depicted in Table 5-3 and Figure 5-8. To obtain an acceptable difference between heads, it is assumed that this difference should remain below 10% of the aquifer thickness:

$$|(Observed\ head - Modeled\ head)| \leq 10\% \times H \qquad \text{Equation 5.1}$$

Table 5-3. Calibration statistics

Number of Observations:	4
Maximum Difference:	1.7
Minimum Difference:	-2.4
Average Difference (AD):	-0.1
Median Difference (MAD):	0.1
Mean Absolute Difference:	1.9
RMS Difference:	1.9

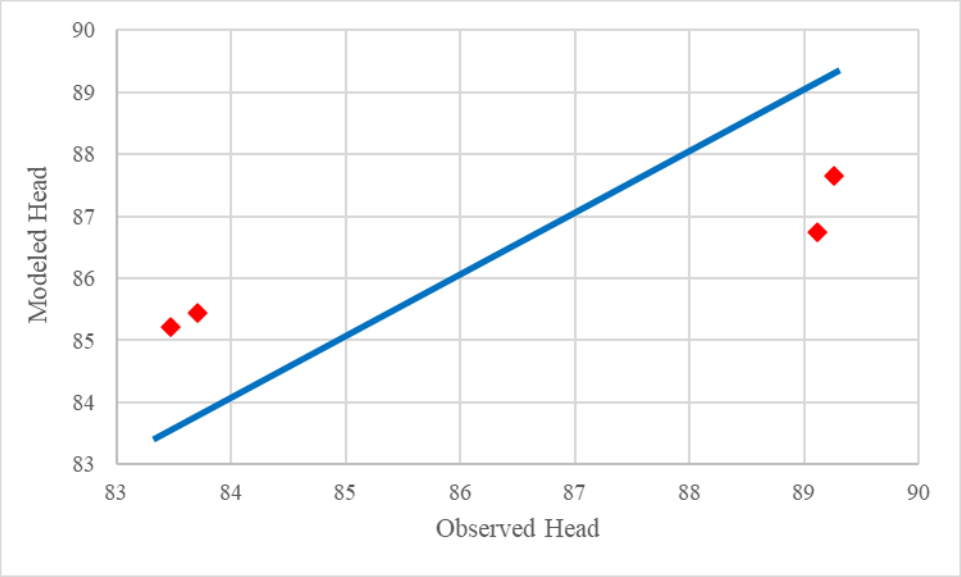

Figure 5-8. Head calibration

By setting the value of H to 17.5 m and adjusting the K parameter to 30.4 m/day, the calibration criteria are met for three of the observations. Subsequently, the results obtained after the calibration process are presented in Table 5-4 and the trace lines for the Håvesten I and II after calibration are depicted in Figure 5-9.

Table 5-4. Residual head after calibration

Observation well	Observed head	Modeled head	Residual
Rb 7803	89.259	87.65021	-1.60879
Rb 7802	89.117	86.74033	-2.37667
Rb 7402	83.709	85.44883	1.73983
Rb 7401	83.474	85.1629	1.74229

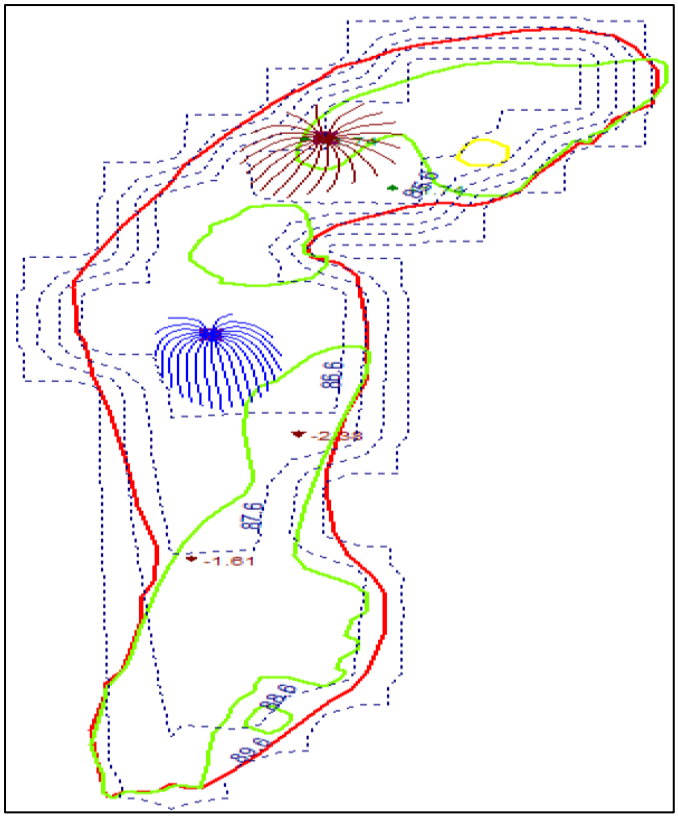

Figure 5-9. Traced particles in WhAEM after the calibration process

5.1.3 Comparison

To effectively assess the impact of uncertainties in the simulation and facilitate a comprehensive comparison of the models, it is crucial to initially evaluate the models by excluding uncertainties. This involves considering only the average values for parameters, enabling confident determination that any subsequent differences observed are solely due to the implementation of uncertainties, rather than being influenced by variations in the models' criteria. The comparison is limited to the results obtained from WhAEM and Scenario 8 of TimML, both of which incorporate the bedrock within the aquifer for a more accurate modeling approach. The comparison between the two models before consideration of uncertainties can be observed in Figure 5-10. Only a marginal difference can be seen between these two models, indicating that the variations observed in the subsequent comparison can be attributed to the consideration of uncertainties rather than inherent disparities between the models.

Figure 5-11 shows the comparison of protection areas generated by the WhAEM and TimML models. The analysis is conducted for a TOT of 1 year, with the WhAEM model utilizing average parameter values and the TimML model incorporating uncertainties. In Table 5-5, the size of protected areas for both models is presented, showcasing the quantitative assessment of the protective coverage provided by each model.

Table 5-5. Comparison between WhAEM and TimML protection area

Method	Area (m^2)
WhAEM	103,899
TimML- 8^{th} scenario without uncertainties	77,986
TimML- 8^{th} scenario with uncertainties	151,423

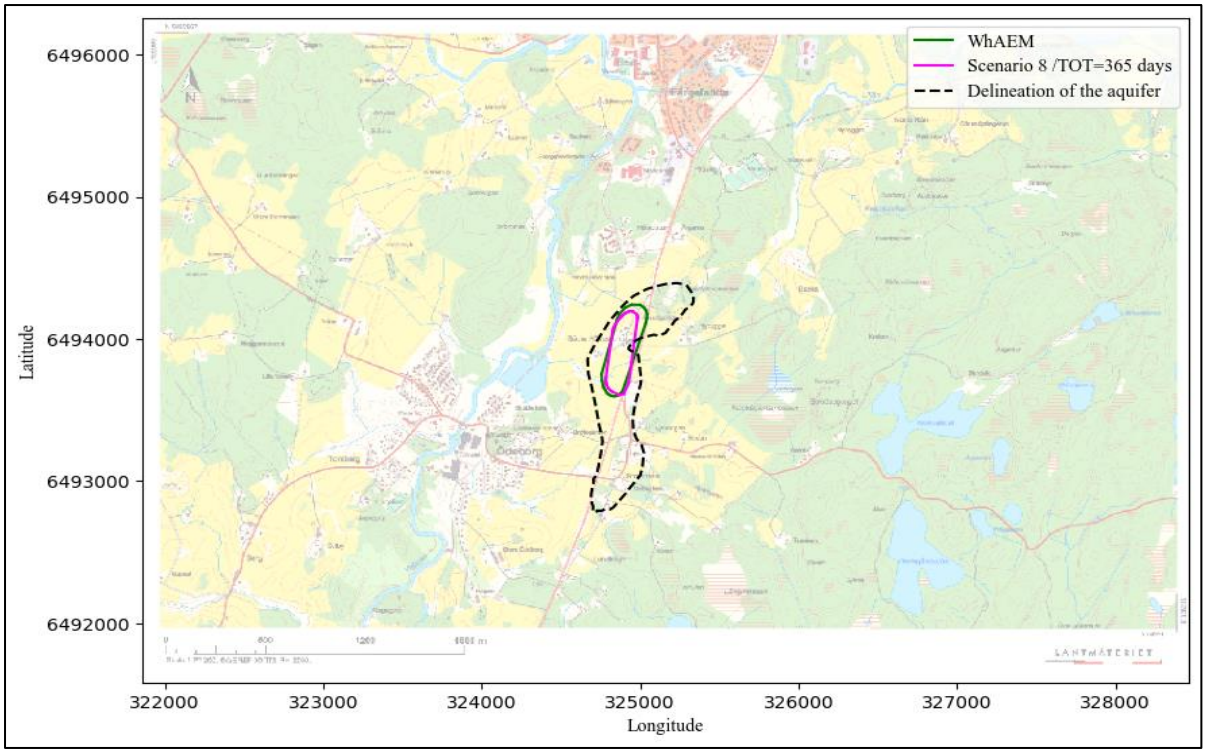

Figure 5-10. Comparison between WhAEM and TimML excluding uncertainties

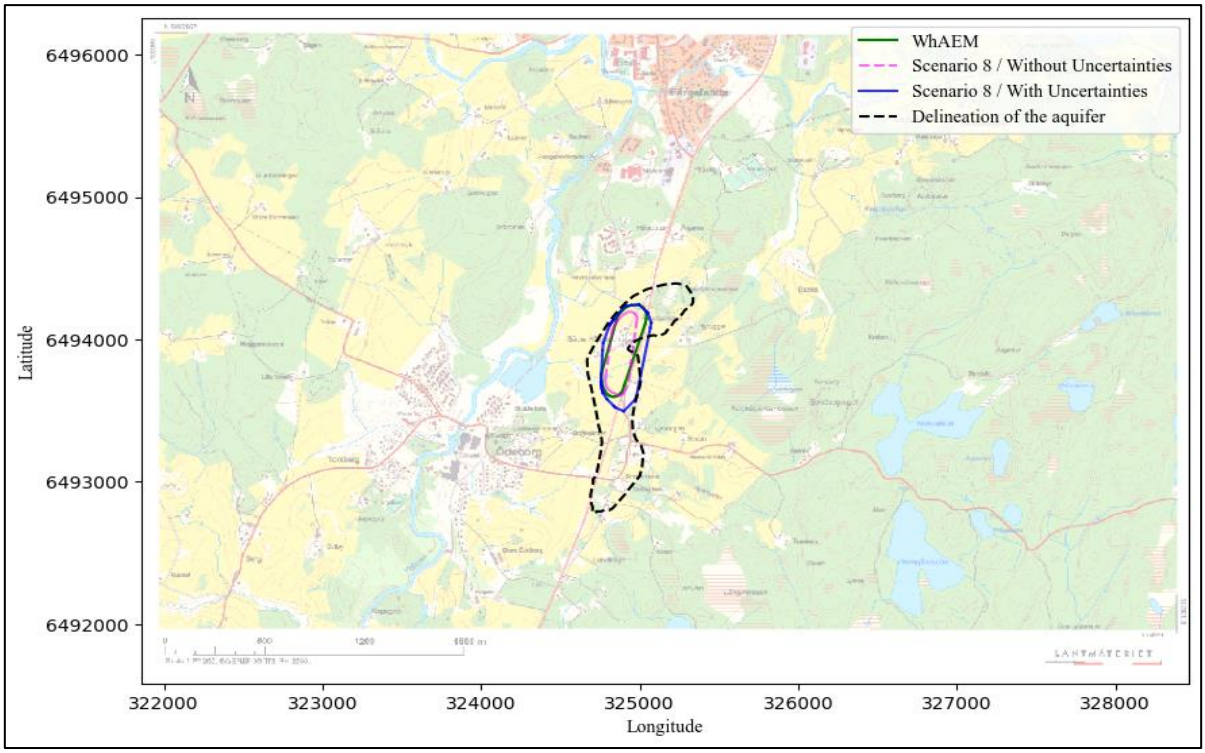

Figure 5-11. Comparison between WhAEM and TimML including uncertainties in the latter model

6

Discussion

This chapter will discuss the results of the study, providing a detailed analysis and interpretation of the findings, and examining their significance in relation to the research objectives. Additionally, it will explore the implications of the results, and address any unexpected outcomes or limitations encountered during the study.

6.1 Application of MCS and TimML integrated model

In this study, an essential development presented is the inclusion of Monte Carlo simulations (MCS) within the TimML code, enabling the consideration of parameter uncertainties in groundwater modeling. The utilization of MCS represents a powerful and effective approach to address these uncertainties. By generating numerous iterations of the model, each incorporating randomly sampled parameter values from their respective distributions, a comprehensive range of possible outcomes can be obtained. This approach enhances the robustness of WHPA estimation, as it accounts for the inherent variability in parameters that significantly influence the modeling results. Consequently, the integration of MCS into the developed TimML model significantly enhances the reliability and accuracy of the modeling outcomes by encompassing the entire spectrum of potential outcomes associated with uncertain parameters.

6.2 Assessing uncertainties in WHPA estimation

The findings of this study demonstrate marginal disparities in the WHPAs obtained from the WhAEM and TimML models when solely considering point estimates of the morel parameters (mean values were applied). These differences can be attributed to multiple factors, such as disparities in calibration approaches, variances in the underlying algorithms and methodologies employed for simulating groundwater flow and calculating WHPAs, and the potential influence of manually defining WHPAs in the WhAEM software. After implementing uncertainties in the model through the integration of MCS with TimML, the results demonstrate that the coverage of the developed integrated model expands twofold compared to the previous version of TimML. Additionally, when compared to WhAEM, the integrated model exhibits a 1.5 times larger coverage of the protection area. The increase in the protection area further emphasizes the importance of considering uncertainties in parameter values, as it has the potential to substantially alter the projected extent of the WHPA.

The analysis demonstrates that conceptual model uncertainties, characterized by varying assumptions regarding geological and hydrogeological interpretations, play a vital role in shaping the modeling outcomes, often leading to substantial changes in results. It underscores the necessity of carefully considering conceptual model uncertainties before delving into the uncertainties associated with specific parameters. The model scenarios considered both model structure and input parameters uncertainties. In this project the latter is addressed through the application of stochastic analysis, specifically Monte Carlo simulation. However, relying solely on this type of analysis may not provide stakeholders with accurate decision-making, as it disregards the importance of model structure uncertainties.

The variations in output among the different scenarios align with the disparities in conceptual models. For instance, when comparing scenarios 7 and 8, the only distinction lies in the inclusion of groundwater delineation as an inhomogeneity. Notably, the head contours in

scenario 7 depict confined aquifers in both Håvesten I and II, deviating from the actual characteristics of the area. This discrepancy is also evident in the 3rd scenario, underscoring the significant influence of conceptual model choices on the simulation results. However, it is important to view these differences not as failures or rejections of the models, but rather as indications of the effectiveness of considering uncertainties in the modeling process, i.e., by testing different conceptual scenarios. In cases where field data is insufficient, a uniform flow model can serve as a reasonable approximation for the area, albeit potentially resulting in an overestimated WHPA. The study's results indicate that scenario 6, which incorporates both uniform flow and heterogeneity within a 0.17 km^2 area, can encompass the WHPA generated by scenario 8, regarded as the reference scenario representing a more realistic model.

However, for areas characterized as highly vulnerable, such as drinking water sources, the allocating of additional resources for data collection becomes crucial to reduce biases in the model structure. Without conducting a sensitivity analysis, it remains challenging to explicitly determine the primary source of uncertainty in the model or identify the parameter that significantly contributes to the variation within each model. Nevertheless, certain observations can still be made regarding the different scenarios examined in the study.

In scenario 1, the trace lines accurately depict the flow direction, which is towards the northeast. The elongated paths observed in this scenario are a result of the absence of barriers obstructing the groundwater flow. Although this scenario does not perfectly represent reality, it offers valuable insights into groundwater behavior. In the 2nd scenario, the implementation of inhomogeneity significantly influences the trace lines. The redirection of groundwater flow occurs due to the substantial contrast between the inner and outer parts of the inhomogeneity. This highlights the crucial role of heterogeneity in shaping the trace lines and emphasizes the importance of carefully considering this factor in the modeling and analysis of groundwater flow, as well as in the delineation of WHPA.

The observed disruptions in the trace lines and flow direction when entering a recharge area with the same hydraulic conductivity and porosity as the surrounding aquifer can be attributed to the variations in algorithms and assumptions used in WhAEM and TimML. In the 4th scenario, the changes in flow direction are not abrupt and can be considered of minimal significance. However, it is important to note that in the 8th scenario, this pattern is specifically observed for Håvesten II and deviates from the trace paths generated by the WhAEM software. These discrepancies highlight the divergent modeling approaches and emphasize the need for careful consideration when interpreting the results of different software applications.

The comparison between scenarios 4 and 8, specifically focusing on Håvesten II, highlights the significant influence of good interactions on flow patterns and alterations in groundwater flow paths. In scenario 4, where the pumping well Håvesten I is absent, the trace lines exhibit a more dispersed distribution throughout the area. Similar comparisons can be made between scenarios 1 and 5, as well as scenarios 2 and 6. The introduction of a new pumping well creates a localized drawdown or hydraulic gradient in the aquifer, subsequently affecting the direction and magnitude of groundwater flow. The extent of this impact is dependent on various factors, including the hydraulic properties of the aquifer, the distance between the wells, pumping rates, and the hydrogeological conditions. It is crucial to consider these factors when assessing the effects of multiple wells on groundwater flow. The interactions between wells can lead to changes in flow paths and the distribution of trace lines, ultimately influencing the overall behavior of the GS.

As mentioned previously, the vertical changes in trace lines observed in this study are primarily attributed to recharge. The model utilized three polygons to represent recharge areas, with two of them situated near Håvesten I. Consequently, the vertical cross-section clearly illustrates the significant impact of recharge on the trace lines on both sides of Håvesten I. The proximity of these recharge areas intensifies the influence of recharge on the distribution and behavior of the trace lines within the aquifer.

Furthermore, it is essential to acknowledge that the pumping well rate possesses the potential to significantly affect the dynamics of aquifer recharge. When pumping occurs, it can alter the overall recharge rate and subsequently influence the vertical distribution of groundwater flow. The combined effects of recharge and pumping create complex interactions, leading to variations in the vertical distribution of groundwater flow within the aquifer. Considering both recharge and pumping is crucial for a comprehensive understanding of the factors influencing the vertical changes in trace lines. The interplay between these processes plays a pivotal role in shaping the behavior and distribution of groundwater flow within the aquifer.

Hence, it is imperative to recognize that assumptions made during the groundwater modeling process introduce uncertainties in the model outputs, underscoring the significance of a strong conceptual understanding of the site. By developing a robust conceptual model based on site-specific knowledge, uncertainties can be effectively narrowed down. When addressing parameter uncertainties, stochastic techniques such as MCS can be employed, utilizing parameter distributions that encompass the associated uncertainties. However, dealing with structural uncertainties in the model presents a challenge due to the vast number of potential models that can be considered, which is impractical to test comprehensively within the constraints of a project, particularly due to resource limitations.

In the context of this study, the exploration of possibilities was limited to eight different scenarios. Although this presents a constrained analysis, it highlights the need for careful management and a thorough understanding of the site-specific conditions to inform the selection of appropriate conceptual models that capture the key characteristics and uncertainties of the system. It should be noted that the limited exploration of scenarios does not imply that these eight scenarios encompass all possible realistic models. Moreover, as previously discussed, two scenarios were found to be inadequate in meeting the specifications of the case study. Rather, the focus was on critically evaluating and identifying a reasonable scenario that aligns with the available data and conceptual understanding of the site. The objective was to identify a scenario that provides useful information and represents a practical approximation of the site conditions for estimating the WHPA.

6.3 Project specific limitations

Data collection for groundwater characteristics often requires borehole excavation and hydraulic tests. Unfortunately, in the selected study site, complete data on the grain size distribution and hydraulic conductivity for the entire area were unavailable. As a result, it was necessary to generalize the existing data from one borehole to the entire region. However, this assumption can significantly impact the results, highlighting the importance of obtaining precise data through various in-situ and laboratory examinations.

The study area encompasses two main aquifers where one is confined and the other is an unconfined aquifer. However, pumping from the confined aquifer, which is the focus of this project, has been halted due to the detection of contamination with an unknown source.

Meanwhile, active pumping continues in the unconfined aquifer. Consequently, the measurements of heads within the study area cannot accurately depict the groundwater behavior during the pumping period.

To simplify the GS, a uniform flow approach has been employed. The hydraulic gradient and flow direction in this method are determined based on the measured heads in the unconfined aquifer, as there are insufficient measurements available in the confined aquifer. This assumption fails to account for the distinct behavior of the confined and unconfined aquifers and disregards the no-pumping conditions within the confined layer. Additionally, the observation wells with head measurements must be drilled in the same geological layer with consistent hydraulic conductivity values, as this ensures more accurate parameter calculations in terms of uniform flow. However, in this case, one of the observation wells is situated outside the groundwater esker, and this offset has been disregarded in the computations.

Another noteworthy limitation of this study lies in the incomplete characterization of the geology of the area. While the available maps provide a clear understanding of the geological formations present, they fail to specify the thickness of individual strata. Consequently, the project's modeling efforts solely encompass the outcrops of bedrock, neglecting the presence of other significant materials. As a result, a comprehensive depiction of the geological composition is not achievable due to the absence of information pertaining to stratum thickness.

As explained in the methodology chapter, an MCS process was employed, generating 100,000 values for the input parameters. However, due to the computational demands of utilizing the entire set of generated values within the TimML groundwater modeling framework, a subset of 100 iterations was selected. This corresponds to randomly choosing 100 samples from the pool of 100,000 generated values to effectively incorporate the MCS approach into TimML.

7

Conclusion & Recommendation

This study set out to evaluate the impact of multiple sources of uncertainty, including parameter and conceptual uncertainties, on WHPA variations in a groundwater modeling problem using AEM. To address parameter uncertainty, TimML code was developed to enable the MCS process. Additionally, eight distinct scenarios were implemented in the TimML to explore different conceptual models. The resulting outcomes were compared against the result obtained from the WhAEM software, which served as a benchmark, considering only average values of input parameters. The comparison revealed that conceptual assumptions introduce significant uncertainties into the model, highlighting their critical influence that cannot be overlooked. Furthermore, focusing solely on addressing parameter uncertainties disregards the importance of model structure uncertainties, which can have a substantial impact on model outcomes.

By acknowledging the dominance of conceptual uncertainties and recognizing the importance of model structure uncertainties, this study emphasizes the need to comprehensively address and incorporate all types of uncertainties in groundwater modeling. The primary focus of this study was to enable the integration of MCS in TimML, specifically to address parameter uncertainties and evaluate their impact on WHPA variations. Through this approach, it is possible to run TimML with uncertainties and derive appropriately defined WHPAs based on the results. This capability provides a valuable tool for capturing the inherent uncertainties in the modeling process and enhancing the accuracy and reliability of WHPA estimations.

In addition to delineating WHPA based on TOT, it is essential to note that the definition of a water protection area should also encompass activities in the area. Therefore, according to the Swedish guidelines (SEPA, 2011), a risk-based approach should be adopted when defining the water protection area. This approach involves considering not only the technical aspects related to groundwater flow and contamination but also the potential activities and their associated risks within the area. By incorporating these factors, a more comprehensive and effective water protection strategy can be developed. Furthermore, despite the additional time and preparation required for AEM compared to fixed or calculated radius methods, it offers high flexibility in handling different boundary scenarios and incorporating uncertainties. This advantage is particularly beneficial in cases where data scarcity exists, which is common in groundwater modeling problems.

7.1 Recommendation for possible improvement in the case study

Based on the experiences and findings from this thesis, several approaches are suggested for the Håvesten aquifer. These approaches, which can be implemented separately or in combination, aim to improve the understanding and management of the aquifer system:

- Further investigation into the interaction between unconfined and confined aquifers, as well as the resultant changes in WHPA, is needed. The decision to combine or separate the WHPA for these aquifer types can significantly impact the outcomes. Therefore, a more comprehensive study is necessary to better understand the implications and potential consequences of such a decision.

- Given the potential for uncertainty associated with simplified methods like uniform flow, it is recommended that efforts to incorporate essential details into the model are not overlooked. While it is acknowledged that such considerations may significantly increase the computational time required and necessitate more powerful computing resources, the benefits of improved accuracy and reduced uncertainty make it a worthwhile pursuit.

- In the context of an AEM, considering multiple conceptual models is crucial to account for uncertainties in the system. To manage the complexity and avoid setting up an excessive number of models, it is recommended to include different hypotheses that have not been disproven by data and are believed to have a substantial influence on the specific modeling objective. By incorporating these pertinent conceptual models and excluding less significant or redundant hypotheses, the overall understanding and analysis of the system can be improved effectively.

- When the model represents a highly vulnerable area, it becomes crucial to gather additional field observations to minimize uncertainties. This approach enhances the accuracy and reliability of the model.

- It is advisable to increase the number of iterations to obtain a more precise and refined result. This iterative process allows for a thorough exploration and adjustment of the model, leading to improved accuracy and confidence in the outcome.

Bibliography

Anderson, M. P., Woessner, W. W., & Hunt, R. J. (2015). *Applied groundwater modeling: simulation of flow and advective transport*. Elsevier.

Badv, K., & Deriszadeh, M. (2005). WELLHEAD PROTECTION AREA DELINEATION USING THE ANALYTIC ELEMENT METHOD. *Water, Air, and Soil Pollution*, *161*, 39–54.

Bakker, M. (2006). An analytic element approach for modeling polygonal inhomogeneities in multi-aquifer systems. *Advances in Water Resources*, *29*(10), 1546–1555. https://doi.org/10.1016/j.advwatres.2005.11.005

Bakker, M., & Kelson, V. A. (2009). Writing analytic element programs in python. *Ground Water*, *47*(6), 828–834. https://doi.org/10.1111/j.1745-6584.2009.00583.x

Bhatt, K. (1993). Uncertainty in wellhead protection area delineation due to uncertainty in aquifer parameter values. In *Journal of Hydrology* (Vol. 149).

Bureau of Reclamation California-Great Basin. (2020). *Water Facts - Worldwide Water Supply*. Central California Area Office (CCAO) - American River Water Education Center (ARWEC). https://www.usbr.gov/mp/arwec/water-facts-ww-water-sup.html

Carey, Mike., Hayes, P., Renner, Axel., & Great Britain. Environment Agency. (2009). *Groundwater source protection zones: review of methods*. Environment Agency.

Craig, J. (n.d.). *The Analytic Element Method*. Retrieved May 19, 2023, from https://www.civil.uwaterloo.ca/jrcraig/pdf/EARTH661_AEMLecture.pdf

Cromer, W. C. (2013, November). *Groundwater principles*. https://www.williamccromer.com/content/uploads/2013/12/Groundwater-principles.pdf

Enemark, T., Peeters, L. J. M., Mallants, D., & Batelaan, O. (2019). Hydrogeological conceptual model building and testing: A review. *Journal of Hydrology*, *569*, 310–329. https://doi.org/10.1016/j.jhydrol.2018.12.007

Fetter, C. W. (2014). *Applied hydrogeology* (Fourth edition). Pearson Education.

Gupta, A., & Ramanathan, A. L. (2019). Grain texture as a proxy to understand porosity, permeability and density in Chandra Basin, India. *SN Applied Sciences*, *1*(1). https://doi.org/10.1007/s42452-018-0001-3

Heath, R. C. (1983). *Basic ground-water hydrology*. U.S. Geological Survey.

H.M. Haitjema. (1995). *Analytic Element Modeling of Groundwater Flow*. Academic Press. https://doi.org/10.1016/B978-0-12-316550-3.X5000-4

Højberg, A. L., & Refsgaard, J. C. (2005). Model uncertainty-parameter uncertainty versus conceptual models. *Water Science & Technology*, *52*, 177–186. https://iwaponline.com/wst/article-pdf/52/6/177/434131/177.pdf

Hunt, R. J. (2006). Ground water modeling applications using the analytic element method. In *Ground Water* (Vol. 44, Issue 1, pp. 5–15). https://doi.org/10.1111/j.1745-6584.2005.00143.x

Kraemer, S. R. , Haitjema, H. M., & Kelson, V. A. (2000). *Working with WhAEM2000: Source Water Assessment for a Glacial Outwash Wellfield, Vincennes, Indiana*. www.miktex.org

Lång, L. O. (2022). *Meeting on Håvesten Aquifer*. Oral consultation from SGU.

Lång, L. O., & Lindh, Å. (2016). *GRUNDVATTENMAGASINET HÅVESTEN*. www.sgu.se

Larum, D. (2021, July 30). *Soil Porosity Information – Learn What Makes Soil Porous*. https://www.gardeningknowhow.com/garden-how-to/soil-fertilizers/soil-porosity-information.htm#:~:text=Soil%20porosity%20usually%20falls%20into,permeability%20and%20water%20holding%20capacity.

Liu, Y., Weisbrod, N., & Yakirevich, A. (2019). Comparative study of methods for delineating the wellhead protection area in an unconfined coastal aquifer. *Water (Switzerland)*, *11*(6). https://doi.org/10.3390/w11061168

Nikiel, M., & Zdechlik, R. (2022). Delineation of wellhead protection area based on the analytical elements method (AEM) – a case study with comparative research. *Geology, Geophysics and Environment*, *48*(4), 335–352. https://doi.org/10.7494/geol.2022.48.4.335

Ramgraber, M., & Schirmer, M. (2021). Hydrogeological Uncertainty Estimation With the Analytic Element Method. *Water Resources Research*, *57*(6). https://doi.org/10.1029/2020WR029509

Raymond, H. A., Bondoc, M., McGinnis, J., Metropulos, K., Heider, P., Reed, A., & Saines, S. (2006). Using analytic element models to delineate drinking water source protection areas. *Ground Water*, *44*(1), 16–23. https://doi.org/10.1111/j.1745-6584.2005.00122.x

SEPA. (2011). *Handbook for water protection areas (in Swedish)*. Swedish Environmental Protection Agency (SEPA).

Sikdar, P. K. (2019). *Groundwater Development and Management Issues and Challenges in South Asia* (Vol. 1). https://doi.org/10.1007/978-3-319-75115-3

SLU University Library. (n.d.). *Find digital maps and geodata*. Retrieved May 21, 2023, from https://zeus.slu.se/get/?drop=

Staboultzidis, A. G., Dokou, Z., & Karatzas, G. P. (2017). Capture zone delineation and protection area mapping in the aquifer of Agia, Crete, Greece. *Environmental Processes*, *4*(1), S95–S112. https://doi.org/10.1007/s40710-017-0221-3

Strack, O. D. L. (1989). *Groundwater mechanics*. Englewood Cliffs, New Jersey: Prentice Hall.

Strack, O. D. L. (2003). Theory and applications of the Analytic Element Method. *Reviews of Geophysics*, *41*(2). https://doi.org/10.1029/2002RG000111

SwAM. (2021). *Guidance on the establishment and management of water protection areas (in Swedish)*. Swedish Agency for Marine and Water Management (SwAM). www.havochvatten.se

The Swedish Research Council Formas. (2009). *Drinking Water-Sources, Sanitation and Safeguarding*.

Theodossiou, N., Latinopoulos, P., & Fotopoulou, E. (2005). APPLICATION OF MONTE CARLO ANALYSIS IN THE DELINEATION OF WELL HEAD PROTECTION AREAS. In *Technology Rhodes island*.

U.S. EPA. (1987). *Guidelines for Delineation of Wellhead Protection Areas*.

U.S.EPA. (1994). *Handbook: Ground Water and Wellhead Protection*.

Van Der Sluijs, J. P., Craye, M., Funtowicz, S., Kloprogge, P., Ravetz, J., & Risbey, J. (2005). Combining quantitative and qualitative measures of uncertainty in model-based environmental assessment: The NUSAP system. *Risk Analysis*, *25*(2), 481–492. https://doi.org/10.1111/j.1539-6924.2005.00604.x

Vaux, H. (2011). Groundwater under stress: The importance of management. *Environmental Earth Sciences*, *62*(1), 19–23. https://doi.org/10.1007/s12665-010-0490-x

VIAK AB. (1978). *HAVESTEN II PROGRAM FÖR UTFÖRANDE AV RÖRBRUNN*.

WHO. (2017). *Guidelines for drinking-water quality*.

Woessner, W. W., & Poeter, E. P. (2020). *Hydrogeologic Properties of Earth Materials and Principles of Groundwater Flow*. The Groundwater Project.

Zhivov, A., Skistad, H., Mundt, E., Posokhin, V., Ratcliff, M., Shilkrot, E., Strongin, A., Li, X., Zhang, T., Zhao, F., Shao, X., & Yang, Y. (2020). Principles of air and

contaminant movement inside and around buildings. In *Industrial Ventilation Design Guidebook: Volume 1 Fundamentals, Second Edition* (pp. 245–370). Elsevier. https://doi.org/10.1016/B978-0-12-816780-9.00007-1

A

Appendix

A.1 Porosity

Total porosity (n) is either equal or less than the effective porosity (n_e) of the sample.

Table A-1. Range of total and effective porosity (Woessner & Poeter, 2020)

	Total Porosity	**Effective Porosity**
Unconsolidated Sediments		
Gravel	0.25 – 0.44	0.13 – 0.44
Coarse Sand	0.31 – 0.46	0.18 – 0.43
Medium Sand		0.16 – 0.46
Fine Sand	0.25 – 0.53	0.01 – 0.46
Silt, loess	0.35 – 0.5	0.01 – 0.39
Clay	0.4 – 0.7	0.01 – 0.18

A.2 Soil profile

Table A-2. Stratigraphy of boreholes (Lång & Lindh, 2016)

Borehole ID	**Reference**	**Longitude (E)**	**Latitude (N)**	**Depth (m)**	**Stratigraphy**
S11072	SGU	324,941	6,493,588	0.0 – 10.4	Stony Gravelly Sand
Rb 7801	VIAK	324,759	6,493,666	0.0 – 11.6	Clay
				11.6 – 12.4	Silt
				12.4 – 14.0	Silty Sand
				14.0 – 16.0	Gravelly Sand
				16.0 – 17.0	Sand
				17.0 – 18.0	Gravelly Sand
				18.0 – 19.5	Gravel
				19.5 – 20.5	Silty Sand
				20.5 – 21.3	Gravel
Rb 7305	VIAK	325,007	6,494,235	0.0 – 6.5	Silty Gravelly Sand
				6.5 – 11.5	Gravelly Sand
				11.5 – 18.3	Gravel
Rb 7307	VIAK	324,732	6,492,968	0 – 5.4	Silty Gravelly Sand
Rb 7804	VIAK	324,843	6,493,778	0 – 10.0	Clay
				10.0 – 13.0	Silt
				13.0 – 19.4	Sand

A.3 Catchment area

The catchment area for groundwater is the area or areas from which precipitation or other water can flow towards the aquifer and recharge it. The outer boundary of the catchment area is often also the boundary for the drainage basin in which the aquifer is located. In the case of the connection of smaller lakes or streams to the groundwater, their entire watersheds are normally included in the catchment area of the aquifer. However, large drainage areas connected to lakes and watercourses are not included. The catchment area can be divided into primary, secondary,

and tertiary parts, depending on whether all or only part of the effective precipitation can be supplied to the aquifer (Lång & Lindh, 2016).

Table A-3. Terminology of catchment area (Lång & Lindh, 2016)

Primary catchment area	The primary catchment area of groundwater is the part or parts of the catchment area where the aquifer is exposed and where the majority or dominant portion of effective precipitation is replenishing the groundwater.
Secondary catchment area	The secondary catchment area of groundwater is part of the catchment area where the aquifer is not exposed and from where the majority or dominant portion of effective precipitation is estimated to contribute to the groundwater.
Tertiary Catchment area	The tertiary catchment area of groundwater includes the parts of the catchment area from which only a portion of the effective precipitation contributes to the aquifer. This can include land areas above or adjacent to the groundwater, from which water leakage to the subsurface water occurs or is estimated to occur under specific conditions (such as groundwater level drawdown or puncturing of sealing layers through construction activities or similar).

A.4 TimML

To execute the TimML code successfully, it is crucial to begin by clearly defining the geology and hydrogeology characteristics specific to the area. Since the code relies on a list of *x* and *y* coordinates for the features, it is essential to supply the model with the precise coordinates of the peripheral points. The position of the aquifer, outcrops of rock, and the recharge areas can be seen in Figure A-1 and a map of these three features together is depicted in Figure A-2.

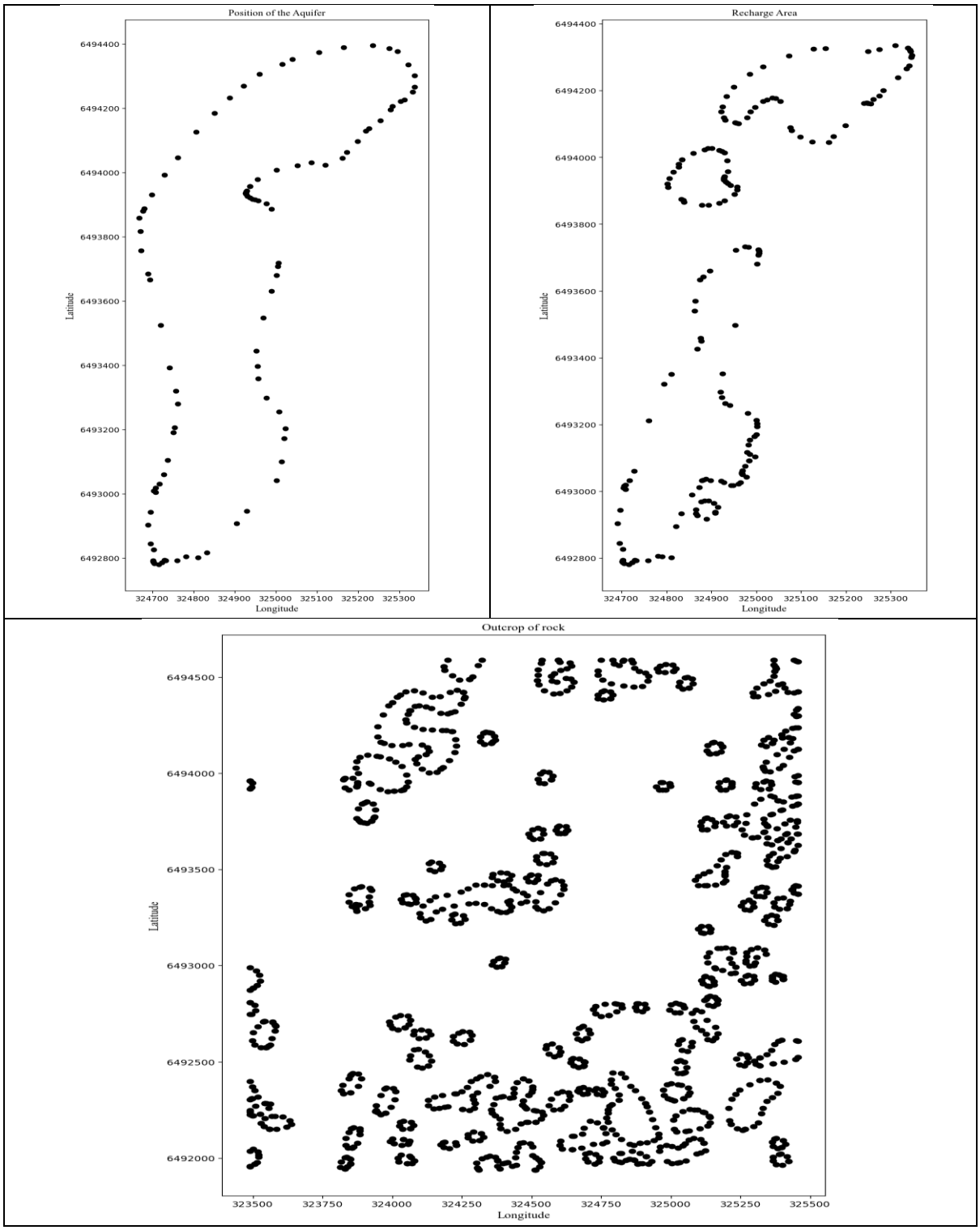

Figure A-1. Coordination of the points creating various features in the study site

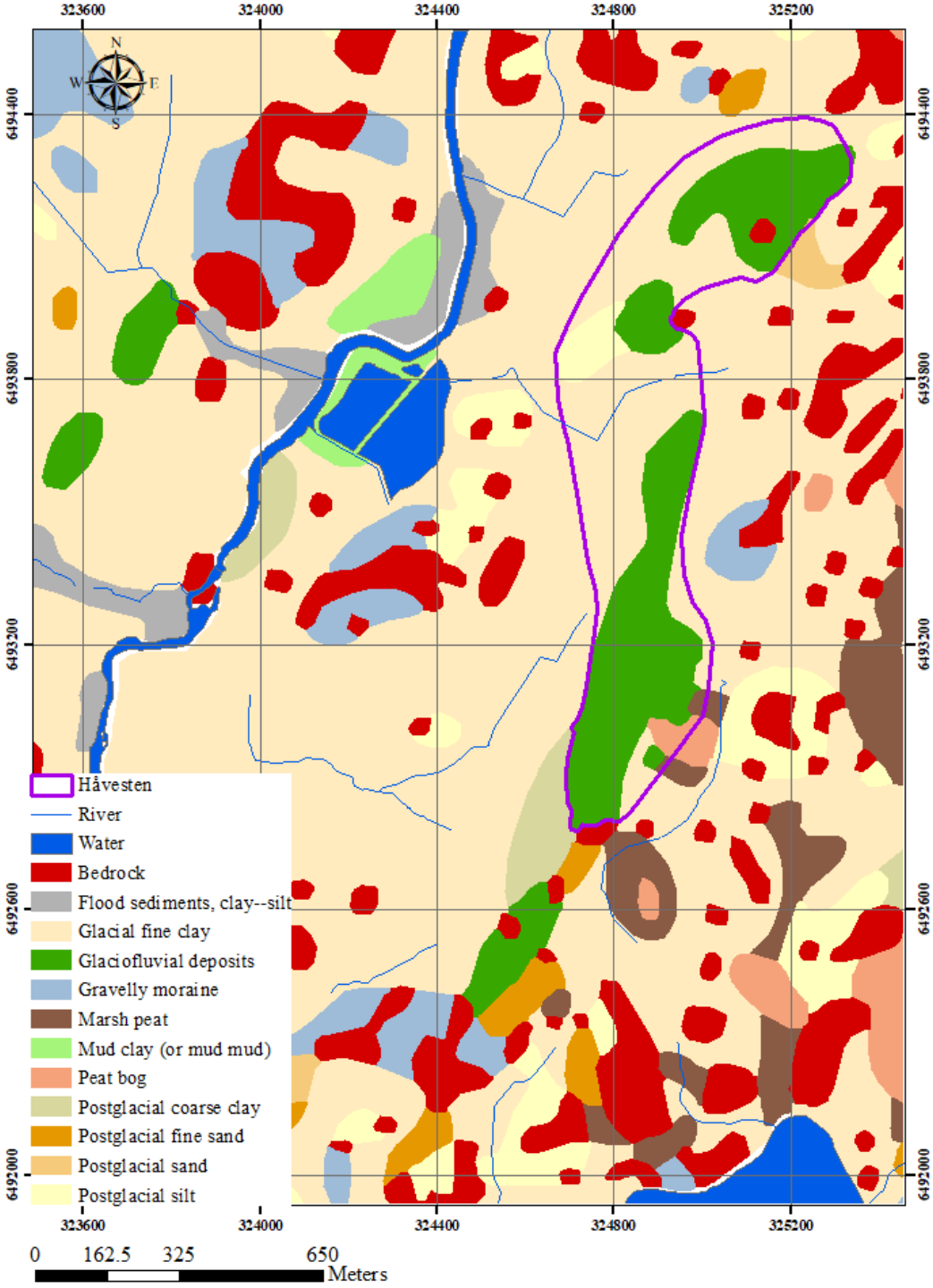

Figure A-2. Detailed geology and hydrogeology of the area

The following steps are required to implement the MCS in TimML:

1. Importing the necessary libraries:

```
import glob
import timml
import numpy as np
import random
import matplotlib.pyplot as plt
```

2. Reading the generated values by MCS and the boundary conditions including the delineation of the aquifer, rock outcrops, and recharge:

```
class Worker:
    def __init__(self, iterations=10) -> None:

        self.aquifer = np.loadtxt("aquifer.txt")
        self.porosity_inputs = np.loadtxt("porosity.txt")
        self.thickness_inputs = np.loadtxt("thickness_values.txt")
        self.k_inputs = np.loadtxt("k_values.txt")
        self.rock = np.loadtxt("Bedrock_*.txt")

        self.recharge = glob.glob("Recharge_*")




        self.num_traces = 20
        self.runs = len(self.k_inputs)

        self.iterations = iterations



        self.rech = [np.loadtxt(o) for o in self.recharge]

        self.figsize = (8, 16)

        self.cur_tail = 0
```

3. Creating the needed elements:
   To represent the aquifer and define its initial parameters, the ModelMaq class is used. For both the delineation of the groundwater and the outcrops of rock the impermeable line doublet is employed (ImpLineDoubleString). Lastly, for the implementation of recharge inhomogeneity is used (PolygonInhomMaq).

```
    def model(self, i):
```

```
        bottom = 72.6347
        thickness = random.choice(self.thickness_inputs)
        top = bottom + thickness
        kaq=random.choice(self.k_inputs)
        npor = random.choice(self.porosity_inputs)

        ml = timml.ModelMaq(kaq=kaq, z=[top, bottom], npor=npor)
        p1 = timml.ImpLineDoubletString(ml, xy=list(zip(self.aquifer[:, 0],
self.aquifer[:, 1])), order=3)
        ld = timml.ImpLineDoubletString(ml, xy=list(zip(self.rock[:, 0],
self.rock[:, 1])), order=3)
        rfRb7802 = timml.Constant(ml, xr=324923.704693, yr=6.493549e+06,
hr=89.177)



        for rech in self.rech:
            r = timml.inhomogeneity.PolygonInhomMaq(ml, xy=list(zip(rech[:,
0], rech[:, 1])), N=531/(1000*365), z=[top, bottom], kaq= kaq, npor= npor)


        w1 = timml.Well(ml, xw=324823.779028, yw=6493755.61435, Qw=250,
rw=0.18, label="Confined well")
        w2 = timml.Well(ml, xw=324954.49775, yw=6494168.45906, Qw=300,
rw=0.18, label="Unconfined well")

        ml.solve()


        ml.plot(win=[324400, 325400, 6492600, 6494600],
                orientation="both",
            figsize=self.figsize,
        )


        trace1 = w1.plotcapzone(
            hstepmax=10,
            nt=self.num_traces,
            zstart=77.6347 ,
            tmax=100,
            orientation="both",
            metadata=True,
            return_traces=True,
        )

        trace2 = w2.plotcapzone(
            hstepmax=10,
            nt=self.num_traces,
```

```
            zstart=77.6347 ,
            tmax=100,
            orientation="both",
            metadata=True,
            return_traces=True,
            color= "C1",
        )

        return trace1, w1, trace2, w2
```

4. Visualization and storing of the outcomes

```
    def run(self):
        all_points1 = []
        all_points2 = []
        tails1 = np.zeros((self.num_traces * self.iterations, 2))
        tails2 = np.zeros((self.num_traces * self.iterations, 2))


        for i in range(self.iterations):

            trace1, w1, trace2, w2 = self.model(i)

            for j in range(self.num_traces):
                points1 = trace1[j]["trace"][:, :3]  # only for x,y,z
                points2 = trace2[j]["trace"][:, :3]
                len_points1 = len(points1)
                len_points2 = len(points2)
                all_points1.append(
                    np.concatenate(
                        [
                            points1,
                            np.array([[i] * len_points1]).T,
                            np.array([[self.cur_tail] * len_points1]).T,
                        ],
                        axis=1,
                    )
                )

                all_points2.append(
                    np.concatenate(
                        [
                            points2,
                            np.array([[i] * len_points2]).T,
                            np.array([[self.cur_tail] * len_points2]).T,
                        ],
                        axis=1,
                    )
                )
```

```
                xs1 = points1[:, 0]
                ys1 = points1[:, 1]
                zs1 = points1[:,2]

                xs2 = points2[:, 0]
                ys2 = points2[:, 1]
                zs2 = points2[:,2]

                distances1 = [(xs1 - w1.xw) ** 2 + (ys1 - w1.yw) ** 2]
                distances2 = [(xs2 - w2.xw) ** 2 + (ys2 - w2.yw) ** 2]

                max_index1 = np.argmax(distances1)
                max_index2 = np.argmax(distances2)

                tails1[self.cur_tail][0], tails1[self.cur_tail][1] =
xs1[max_index1], ys1[max_index1]
                tails2[self.cur_tail][0], tails2[self.cur_tail][1] =
xs2[max_index2], ys2[max_index2]
                self.cur_tail += 1


            # save x and y and z of tracelines to a file
        points_to_save1 = np.concatenate(all_points1)
        points_to_save2 = np.concatenate(all_points2)
        np.savetxt("tails_confined_primary.txt", tails1, fmt="%.3f")
        np.savetxt("tracepoints_ confined.txt", points_to_save1,
fmt="%.3f")
        np.savetxt("tails_unconfined_primary.txt", tails2, fmt="%.3f")
        np.savetxt("tracepoints _unconfined.txt", points_to_save2,
fmt="%.3f")


Worker().run()
```

A.5 Monte Carlo Simulation

A.5.1 Distribution Type

A comparison between normal and log-normal distributions, as the most probable types of governing distributions for hydraulic conductivity, is carried out. In most cases, a log-normal distribution can be a more appropriate representative in a small-scale case and as the area of the study grows further, a normal distribution can lead to more accurate results. In this project, due to a lack of data, comparing the two types of distribution is inevitable.

The following steps are required to find the best-fitted distribution:

- Step 1: Finding the needed statistical parameters such as sample mean value, sample standard deviation, coefficient of variation, etc.
- Step 2: Create functions to calculate the share, sigma, log, and natural log.

- Step 3: Determine action goals and risk of error.
- Step 4: Calculation of the sample mean and standard deviation after logarithmization.
- Step 5: Computation of the statistical interface for both normal and log-normal distribution.
- Step 6: Visualization of the results to find the best fit.
- Step 7: Calculation of the population standard deviation based on a 95% confidence interval of the sample mean value (Equation 4.1).

To find the type of distribution for the available K values, the code is implemented in Python using the Excel method developed by Chalmers University.

1. Import required modules and libraries into Python.

```
import numpy as np
import matplotlib.pyplot as plt
from scipy.stats import norm, lognorm
import statistics
from scipy import stats
import pandas as pd
import seaborn as sns
```

2. Make an array of the available hydraulic conductivities based on Table 4-1.

```
# The data below is based on *10**(-3) m/s
k= np.array([0.07, 0.25, 0.27, 0.25, 0.56, 0.95, 0.06, 1.04, 1.06])
# In Timml the unit for k values is m/d
k_timml= k*(10**-3)*60*60*24
```

3. Finding the required statistical parameters

```
m = statistics.mean(k_timml) # average
s = statistics.stdev(k_timml) # standard deviation
cv = s/m # Coefficient of variation
N = len(k_timml) # Number of analysis data
Min = min(k_timml) # minimum
p25 = np.percentile(k_timml, 25) # 25th percentile
p50 = np.percentile(k_timml, 50) # Median
p75 = np.percentile(k_timml, 75) # 75th percentile
Max = max(k_timml) # maximum
```

4. Creating a data frame for the K values

```
df = pd.DataFrame(data= k_timml, columns=["Data"],
                  index= np.arange(1, len(k_timml) + 1))
df["Sorted Data"]= np.sort(k_timml)
df["Index"] = np.arange(1, len(k_timml) + 1)
```

5. Creating functions to calculate required parameters

```
def share(data, counter):
    if data == 0:
        return "None"
    else:
        return ((counter-0.5)/N)

def sigma(data, share):
    if data == 0:
        return "None"
    else:
        return norm.ppf(share)

def logx (sorted_data):
    if sorted_data == 0:
        return "None"
    else:
        return np.log10(sorted_data)

def natural_log(data):
    if data > 0:
        return np.log(data)
    return False
```

The results can be seen as follows:

Table A-4. The logarithm of the hydraulic values

Index	Data	Sorted Data	Share	Sigma	Log(xi)	LN
1	6.048	5.184	0.055556	-1.593219	0.714665	1.799728
2	21.600	6.048	0.166667	-0.967422	0.781612	3.072693
3	23.328	21.600	0.277778	-0.589456	1.334454	3.149654
4	21.600	21.600	0.388889	-0.282216	1.334454	3.072693
5	48.384	23.328	0.500000	0.000000	1.367878	3.879169
6	82.080	48.384	0.611111	0.282216	1.684702	4.407694
7	5.184	82.080	0.722222	0.589456	1.914237	1.645577
8	89.856	89.856	0.833333	0.967422	1.953547	4.498208
9	91.584	91.584	0.944444	1.593219	1.961820	4.517257

6. Action goals and risk of error

```
ac = float(input("Enter action targets in the form of a percentage: "))
alpha = float(input("Enter maximum error risk: "))
# State the risk that the true value is outside the (two-sided) confidence
interval that you are prepared to take.
# An action target of 15% is considered
# To calculate UCLM 95%, the value 0.10 must be entered as alpha.

n_plus = sum(df.Data > ac) # Number of samples > action target
n_minus = N - n_plus # Number of samples < action target
n_plus_N= n_plus/N # Number of samples > action target
```

7. Statistical inference for normal distribution

```
uclm95 = m + stats.t.ppf(1-alpha/2, N-1)*s/N**0.5
# UCLM = Upper Confidence Limit of the Mean.
lclm95 = m - stats.t.ppf(1-alpha/2, N-1)*s/N**0.5
# LCLM = Lower Confidence Limit of the Mean.
share_to_target = 1-norm.cdf(ac, m, s) # Share > action target
```

8. Statistical inference for log-normal distribution

```
m_log = statistics.mean(df["LN"]) # average
s_log = statistics.stdev(df["LN"]) # standard deviation
median_log = np.exp(m_log)
average_log = np.exp(m_log + s_log**2/2)
sd_log = average_log * (np.exp(s_log**2)-1)**0.5
# Chebyshev UCLM
uclm_log = m + (2/alpha-1)**0.5* sd_log/(N**0.5)
share_to_target_log = 1-lognorm.cdf(ac, s= s_log, scale = np.exp(m_log))
```

9. Finally, for the visualization and comparison graphs are created.

A.5.2 Generating values by MCS

To create the Monte Carlo simulation the mean value (avg) and standard deviation (std_dev) of the input parameter is needed as well as the number of iteration and the type of distribution.

1. Import required modules and libraries into Python.

```
import numpy as np
import scipy.stats as stats
import seaborn as sns
import matplotlib.pyplot as plt
import pandas as pd
sns.set(style="whitegrid")
```

2. Defining the number of iterations

```
num_simulations= 100000
```

3. Monte Carlo Function

```
def monte_carlo_simulation(avg, std_dev, iteration):
    montecarlo_inputs = np.zeros(iteration)
    for i in range(iteration):
        montecarlo_input= np.random.normal(avg, std_dev, 1).round(3)
        while montecarlo_input < 0:
            montecarlo_input= np.random.normal(avg, std_dev, 1).round(3)
        montecarlo_inputs[i]= montecarlo_input
    return montecarlo_inputs
```

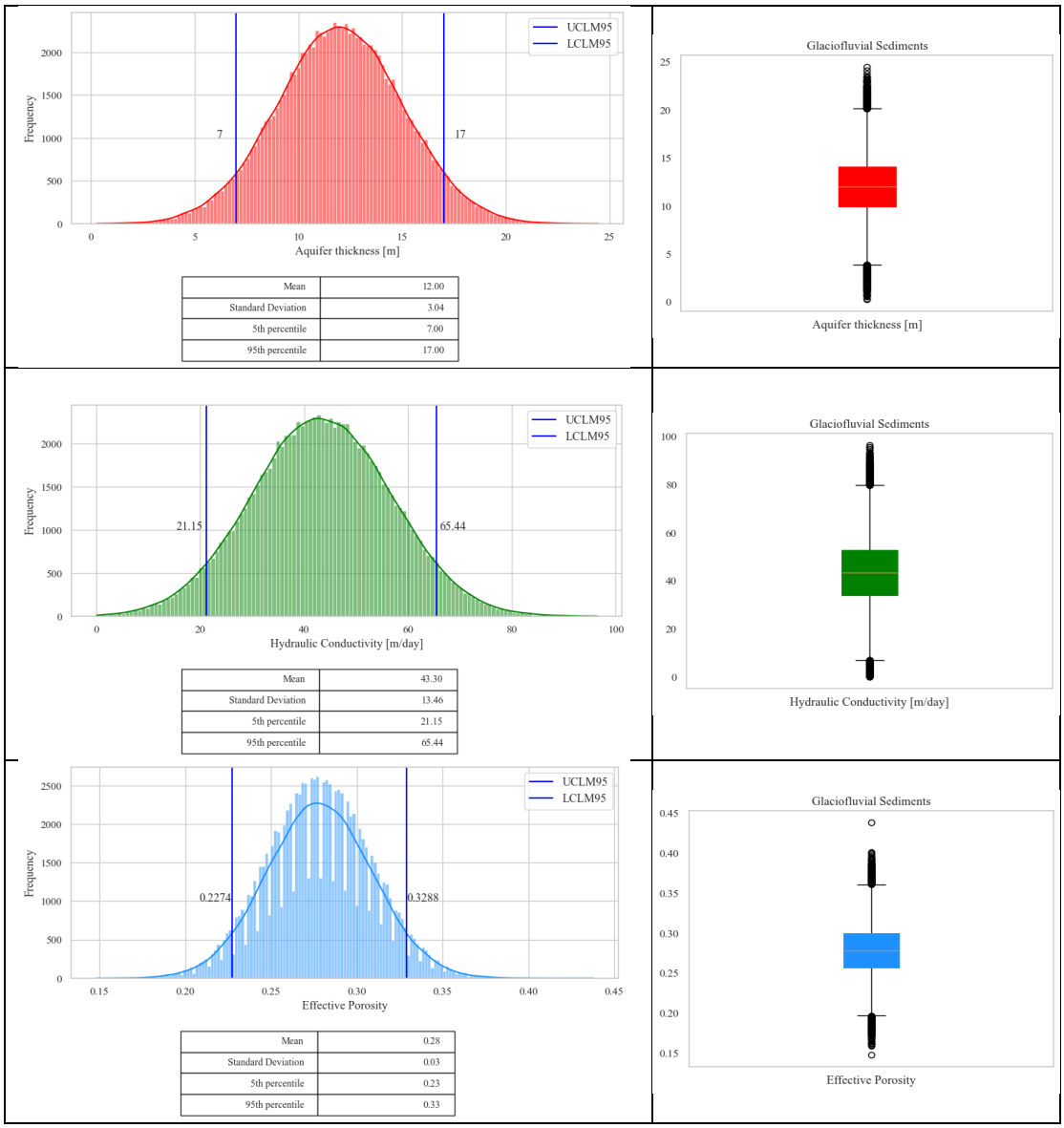

Figure A-3. Histogram and boxplot of the parameters' generation using MCS

A.6 Goodness of fit

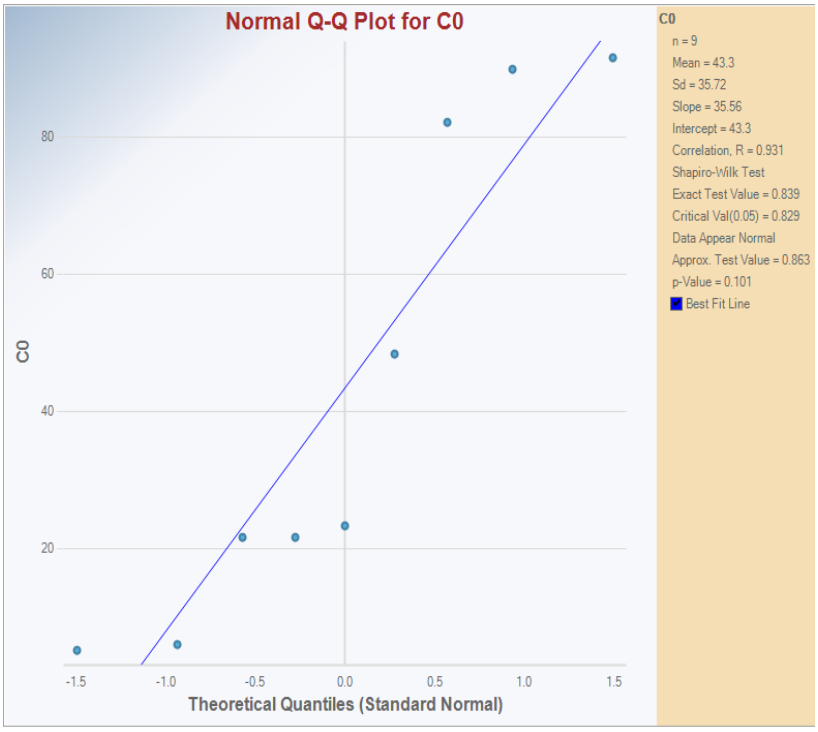

(a)

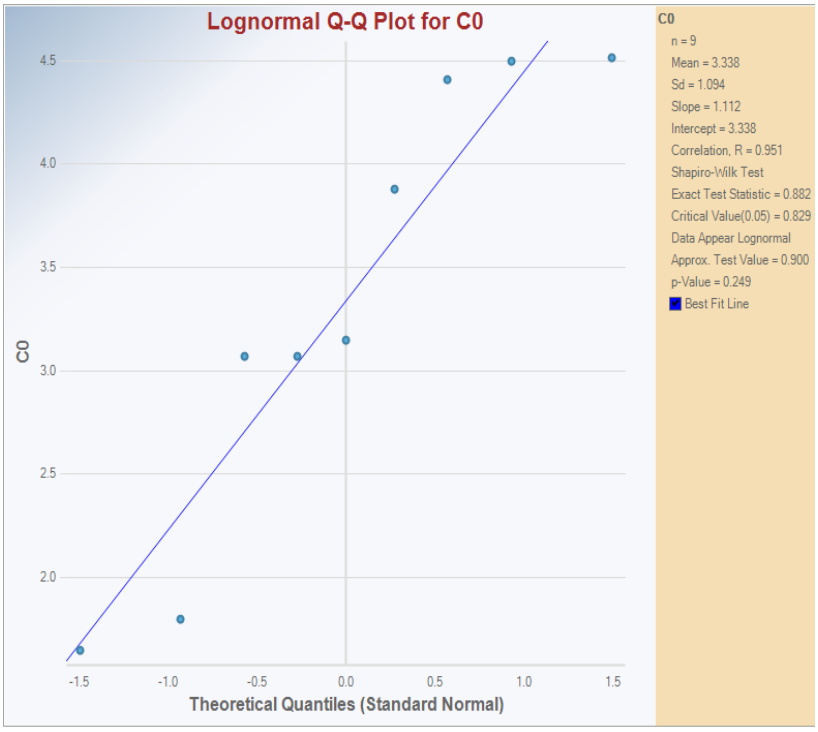

(b)

Figure A-4. The goodness of fit test for hydraulic conductivity using ProUCL

DEPARTMENT OF ARCHITECTURE AND CIVIL ENGINEERING
CHALMERS UNIVERSITY OF TECHNOLOGY
Gothenburg, Sweden 2023
www.chalmers.se

CHALMERS
UNIVERSITY OF TECHNOLOGY